

**SEMMELWEIS EGYETEM**  
**DOKTORI ISKOLA**

**Ph.D. értekezések**

**3159.**

**DEÉZSI-MAGYAR NÓRA**

**Nép- és közegészségtudományok**  
című program

Programvezető: Dr. Ács Nándor, egyetemi tanár  
Témavezető: Dr. Kis Zoltán, tudományos munkatárs

**REVEALING THE *IN VITRO* GROWTH-ADAPTIVE CHANGES OF  
CRIMEAN-CONGO HEMORRHAGIC FEVER VIRUS  
AND CONDUCTING THE FIRST COUNTRY-WIDE  
SEROSURVEILLANCE AMONG HUMANS AND ANIMALS IN  
HUNGARY**

PhD thesis

**Nóra Deézi-Magyar**

Health Sciences Division

Semmelweis University Doctoral School



Supervisor:

Zoltán Kis, PharmD, PhD

Official reviewers:

Zoltán László Tarján, PhD

Béla Kádár, MD, PhD

Head of the Complex Examination Committee:

Károly Nagy, MD, PhD

Members of the Complex Examination Committee:

Katalin Kristóf, MD, PhD

Valéria Endrész, PhD

Budapest

2025

## Table of Contents

List of abbreviations .....	4
1. Introduction .....	7
1.1. The Crimean-Congo hemorrhagic fever virus: taxonomy and discovery .....	7
1.2. Genetic properties and virus structure.....	7
1.3. Genetic diversity .....	9
1.4. Pathogenicity .....	10
1.5. Epidemiology .....	11
1.6. Diagnosis and treatment.....	15
2. Objectives.....	17
3. Materials and methods .....	18
3.1. Cell cultures .....	18
3.2. Virus strain and propagation .....	18
3.3. Serial passaging and virus growth kinetics .....	18
3.4. Nucleic acid extraction and RT-qPCR.....	19
3.5. Infective titration .....	19
3.6. Whole genome sequencing (WGS).....	20
3.7. Sample selection for the human serosurveillance.....	20
3.8. Sample selection for the animal serosurveillance.....	21
3.9. Serological testing.....	21
3.9.1. Screening the human serum samples .....	21
3.9.2. Screening the animal serum samples .....	22
3.10. Data analysis .....	23
3.10.1. Virus growth kinetics .....	23
3.10.2. Whole genome analysis and variant call.....	24
3.10.3. Descriptive analysis and geographical distribution: human serosurveillance.....	24
3.10.4. Descriptive analysis and geographical distribution: animal serosurveillance.....	24
4. Results.....	26
4.1. <i>In vitro</i> growth-induced adaptation to cell lines .....	26
4.1.1. MOI-dependent virus growth kinetics .....	26

4.1.2. Effect of serial passaging and cell line on the virus growth and permissivity .....	28
4.1.3. Growth-induced variant distribution in the viral genome .....	29
4.1.4. Analysis of nucleotide change preferences .....	34
4.1.5. Annotation of consensus level mutations .....	35
4.2. Human serosurveillance .....	39
4.2.1. Study population, sample selection, and data collection.....	39
4.2.2. Serological screening .....	39
4.2.3. Descriptive analysis .....	41
4.2.4. Geographical distribution .....	41
4.3. Animal serosurveillance .....	42
4.3.1. Sample pooling and screening.....	42
4.3.2. Geographical distribution .....	45
5. Discussion .....	48
5.1. In vitro growth-induced adaptation to cell lines .....	48
5.2. Human and animal serosurveillance.....	52
6. Conclusions .....	56
7. Summary .....	58
8. References .....	59
9. Bibliography of publications .....	73
10. Acknowledgements .....	77
11. Appendix .....	78
11.1. Figures.....	78
11.2. Tables .....	83

## List of abbreviations

aa	amino acid
ANOVA	analysis of variance
BHK-21 cells	baby hamster kidney – 21 cells
BSL	biosafety level
CCHF	Crimean-Congo hemorrhagic fever
CCHFV	Crimean-Congo hemorrhagic fever orthonairovirus ( <i>Orthonairovirus haemorrhagiae</i> )
CDC	Centers for Disease Control and Prevention
cDNA	copy DNA
CI	confidence interval
CPE	cytopathic effect
DIC	disseminated intravascular coagulation
DIP	defective interfering particle
DMEM	Dulbecco-modified Eagle medium
DNA	deoxyribonucleic acid
dpi	day post infection
ECACC	European Collection of Authenticated Cell Cultures
ECDC	European Centre for Disease Prevention and Control
ELISA	enzyme-linked immunosorbent assay
EMMa	European Map Maker
ER	endoplasmic reticulum

EVA	European Virus Archive
FBS	fetal bovine serum
FITC	fluorescein isothiocyanate
GMEM	Glasgow Minimum Essential Medium
GPC	glycoprotein precursor complex
GP38	glycoprotein 38
IgG	immunoglobulin G
IgM	immunoglobulin M
IIFA	indirect immunofluorescent assay
kDa	kilodalton
LDLR	low-density lipoprotein receptor
MDBK cells	Madin-Darby Bovine Kidney cells
MOI	multiplicity of infection
NAAT	nucleic acid amplification test
NBL	National Biosafety Laboratory
NCPHP	National Center for Public Health and Pharmacy
NCR	non-coding region
NGS	next generation sequencing
NP	nucleoprotein
nt	nucleotide
NSm	non-structural S protein
NSs	non-structural M protein

NUTS	nomenclature of territorial units for statistics
ORF	open reading frame
PBS	phosphate-buffered saline
PBST	phosphate-buffered saline + Tween20
RdRp	RNA-dependent RNA polymerase
RG	risk group
RNA	ribonucleic acid
rNP	recombinant nucleoprotein
RT-PCR	reverse-transcription polymerase chain reaction
RT-qPCR	real-time reverse-transcription polymerase chain reaction
RSCU	relative synonymous codon usage
SD	standard deviation
SISPA	sequence-independent single primer amplification
SNP	single nucleotide polymorphism
SW13 cell	Scott and White No. 13 cell
TCID50	tissue culture infectious dose 50%
VF	variant frequency
vRNA	viral RNA
WGS	whole genome sequencing
WHO	World Health Organization
ZF	zinc finger

## 1. Introduction

### 1.1. The Crimean-Congo hemorrhagic fever virus: taxonomy and discovery

The *Nairoviridae* virus family belonging to the order *Harevirales* consists of eight genera including the *Orthonairoviruses* that are important human pathogens. Among the 51 species within the *Orthonairovirus* genus, the most significant is the Crimean-Congo hemorrhagic fever serogroup, including the *Orthonairovirus haemorrhagiae* species (historically called as Crimean-Congo hemorrhagic fever orthonairovirus; CCHFV) [1, 2].

CCHFV was first identified in the Crimean Peninsula in the 1940s in patients with hemorrhagic symptoms. In 1944, ticks were confirmed to play an important role in virus transmission as vectors. In 1965, the virus was also isolated in the territory of the Democratic Republic of the Congo. In 1969, it was confirmed that the two virus strains are identical and were named Crimean-Congo hemorrhagic fever virus [3]. Since 2015, CCHFV has been identified as one of the most significant emerging tick-borne pathogens, and was categorized as a priority disease with pandemic potential listed by the World Health Organization (WHO) [4].

### 1.2. Genetic properties and virus structure

CCHFV virions are enveloped, spherical, approximately 100 nm in diameter, and have a host cell-derived lipid envelope [1, 2, 5, 6]. The viral genome consists of three circular RNA segments of negative polarity with complementary non-coding regions present at the 5' and 3' termini of the segments functioning as viral promoters (Figure 1) [5, 6]. Non-coding regions (NCRs) facilitate the binding of RNA-dependent RNA polymerase (RdRp or L protein) to the viral genome during replication, thereby initiating viral transcription and replication. NCRs function to initiate the encapsidation, transcription, replication and genome packaging. The small segment (S; 1.6 kb) encodes the nucleocapsid protein (NP) and the non-structural S protein (NS<sub>S</sub>). The NS<sub>S</sub> is encoded in the opposite orientation relative to the NP gene, indicating that CCHFV might be considered an ambisense virus. The size of

the NP is 54kD and its main role is during virus replication: the NP together with the viral RNA (vRNA) and the RdRp (459 kDa) encoded by the large segment (L; 12.1 kb) form the ribonucleoprotein. In terms of its spatial structure, the L protein is most comparable to the right hand with "finger", "palm" and "thumb" domains. The palm domain contains four main conserved motifs (A-D), of which the active center responsible for polymerase activity is located on domain C. On the surface of the virion, the mature glycoproteins (Gc and Gn) are present, which are responsible for the receptor binding and virus entry. Gn and Gc are encoded by the medium segment (M; 5.4 kb) in a single open reading frame (ORF) as one glycoprotein complex (GPC) that is processed post-translationally into several structural and non-structural proteins. The name Gn refers to the terminal end of the protein with an amino group, located on the surface of the virion, while Gc denotes the end containing the carboxyl group of the glycoprotein, embedded in the lipid envelope of the virus. The non-structural protein encoded on the M segment (NSm) is also produced during the posttranscriptional cleavage of the GPC. NSm is responsible for virus "motion", and it also serves as a virulence factor by potentially increasing viral fitness, pathogenicity in humans and persistence in tick reservoirs [5-8].

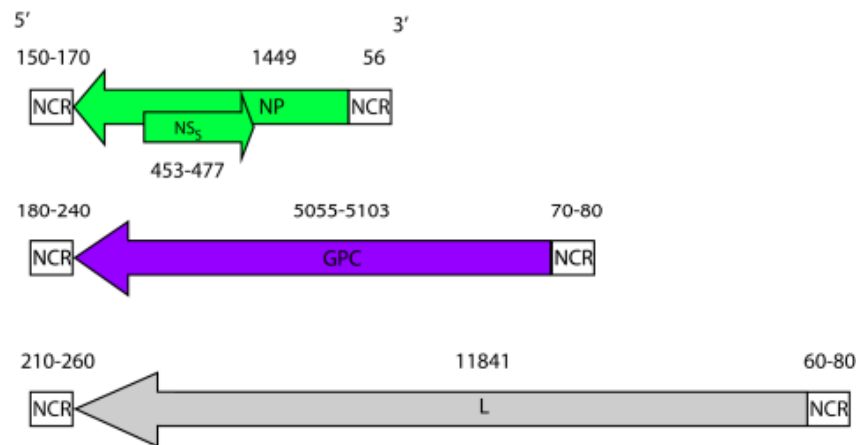


Figure 1. The three genome segments (S, M and L) of the CCHFV [7].

### 1.3. Genetic diversity

In correspondence with the wide geographical distribution, CCHFV is a genetically diverse virus. Although the NP and L proteins are conserved among all CCHFV strains with approximately 95% amino acid identity, the GPC is much variable with less than 75% amino acid conservation [5, 6].

Genetic clades of CCHFV separate based on geographical location, however, the nature of the selective pressures driving this diversity is still unknown [5, 6]. According to phylogenetic analysis of the S segment, CCHFV is divided into seven genetic clades: two lineages originate from Asia, two from Europe, and three from Africa [9]. The mutation rates were estimated to be 1.09E-04, 1.52E-04 and 0.58E-04 substitutions/site/year for the S, M, and L segments, respectively [10].

Inter- and intra-host genetic diversity of RNA viruses, such as CCHFV can be described by the complex interactions between *de novo* mutations and selection that includes adaptation mutations to the host organism, thereby allowing the virus to evade host immunity. A frequently used method to study virus diversity is through mutation accumulation experiments, which involve propagating the virus over many generations intervened with severe bottlenecks in order to reduce the effectiveness of selection. Consequently, mutations within the virus genome can accumulate at the virus-specific unbiased basic mutation rate. One very commonly used bottleneck is infecting the susceptible cells at a very low MOI (multiplicity of infection; the ratio between the infective virus particles and the cells), as it promotes the selection for the fittest genomes within a viral cloud [11]. Codon usage bias as a descriptive phenomenon regarding the evolutionary characteristics of the CCHFV was analyzed by Rahman *et al.* Based on the relative synonymous codon usage (RSCU) and other indicators, the codon usage bias of CCHFV was shown to be relatively low. However, the comparative analysis between the RSCU of CCHFV and the host suggests that the virus tends to evolve to the host's codon usage pattern [12].

#### 1.4. Pathogenicity

The incubation period for the development of symptoms in humans depends on the mode of exposure. Following tick bite, the incubation period generally lasts from 1-3 days (up to 9 days) whereas, the incubation period is 5-6 days with a maximum of 14 days following transmission from infected body fluids [3, 7, 13].

The entry receptor for CCHFV was recently discovered to be the low-density lipoprotein receptor (LDLR) [14, 15]. After the attachment, the virus enters the cell via clathrin-mediated endocytosis [14]. Primary transcription from the vRNA occurs by using host-cell-derived primers and the virus-associated RdRp. Then, translation of the three genome segments occurs along with the co-translational cleavage of the M segment polyprotein and the post-translational cleavage of the precursors. Dimerization of Gn and Gc takes place in the endoplasmic reticulum (ER). After the membrane-associated RNA replication (synthesis and encapsidation of the copy RNA that serves as a template for vRNA synthesis), the dimerized Gn and Gc are transported to the Golgi apparatus, where the newly synthesized NP is localized and the virus assembly takes place. The modified host-membrane is acquired by budding into the Golgi cisternae. After the vesicular transport and virus maturation, the cytoplasmic vesicles containing the virions fuse with the plasma membrane and the mature virus particles are released from the cell [5].

CCHFV infection can cause a wide range of symptoms. In certain hyper-endemic areas, such as Turkey and the Balkan region, the rate of asymptomatic infection is estimated around 80% [3, 13, 35]. In the case of symptomatic infection, the incubation phase is followed by the pre-hemorrhagic phase lasting for 2-4 days, with abrupt onset of nonspecific symptoms such as fever, headache, myalgia, dizziness, neck pain and stiffness, sore eyes and photophobia, sore throat, abdominal pain, nausea, vomiting, and diarrhea [3, 13]. The subsequent hemorrhagic stage is typically short (2-3 days), presenting with petechiae and extended ecchymoses on the mucous membranes and skin. In addition to these symptoms, hemorrhaging from the gums, nose, internal organs, and gastrointestinal system may occur. Severe cases are marked by the rapid progression of disseminated intravascular coagulation (DIC), excessive bleeding, multi-organ failure, and shock. In fatal cases, death typically occurs in the second

week of illness. In survivors, convalescence begins approximately 9 days after symptoms onset [13]. It is estimated, that the case fatality rate among patients seeking hospital treatment is around 5-40% [3, 13]. Due to the expanding geographical distribution of CCHFV, the number of annual cases and seroprevalence are increasing worldwide [3]. Considering the high risk posed by CCHFV infection to the individual and the community, and as there is no licensed vaccination or treatment available, CCHFV is categorized as a risk group 4 (RG4) pathogen, and must be handled under biosafety level 4 (BSL-4) conditions.

### 1.5. Epidemiology

CCHFV is endemic to the Balkan region, Eastern and Southern Europe, the Middle East, Africa and Asia [16]. Over 30 tick species have been described as potential virus carriers worldwide (*Hyalomma spp*, *Rhipicephalus spp*, *Ornithodoros spp*, *Dermacentor spp*, *Ixodes spp ticks*, *Ambylomma variegatum*, *Boophilus decoloratus*, etc.) [17, 18], but the predominant vectors are the ticks of the *Hyalomma* genus (*H. marginatum*, *H. truncatum*, *H. impeltatum*, *H. impressum*, *H. lusitanicum*, etc.) distributed up to the 50° North latitude (Figure 2) [19].

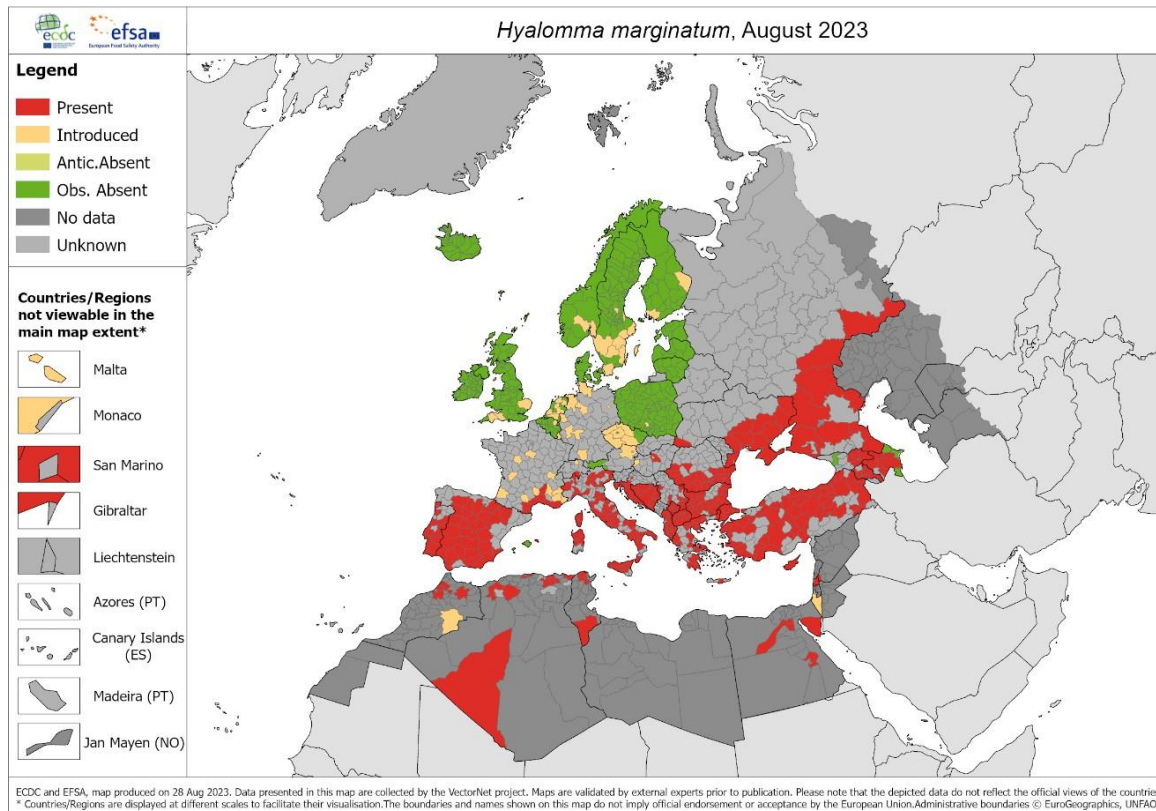


Figure 2. The latest map (2023) on the geographic distribution of the *H. marginatum* tick, the predominant vector of the CCHFV [19].

The natural cycle of CCHFV includes trans-ovarial and trans-stadial transmission among ixodid ticks and involve different wild and domestic animals, such as hares, rodents, cattle, sheep, goats, etc. (Figure 3). The role of animals as virus reservoirs and source of infection has been highlighted by many publications reporting the presence of asymptomatic viremia lasting up to 7–15 days [20, 21, 27]. As CCHFV is maintained through a tick-vertebrate-tick transmission cycle, the major route for human infection is through tick bite or direct exposure to body fluids of infected animals, including removing infected ticks from animals. Human-to-human transmission can also occur, especially as a nosocomial infection (Figure 3) [22-27].

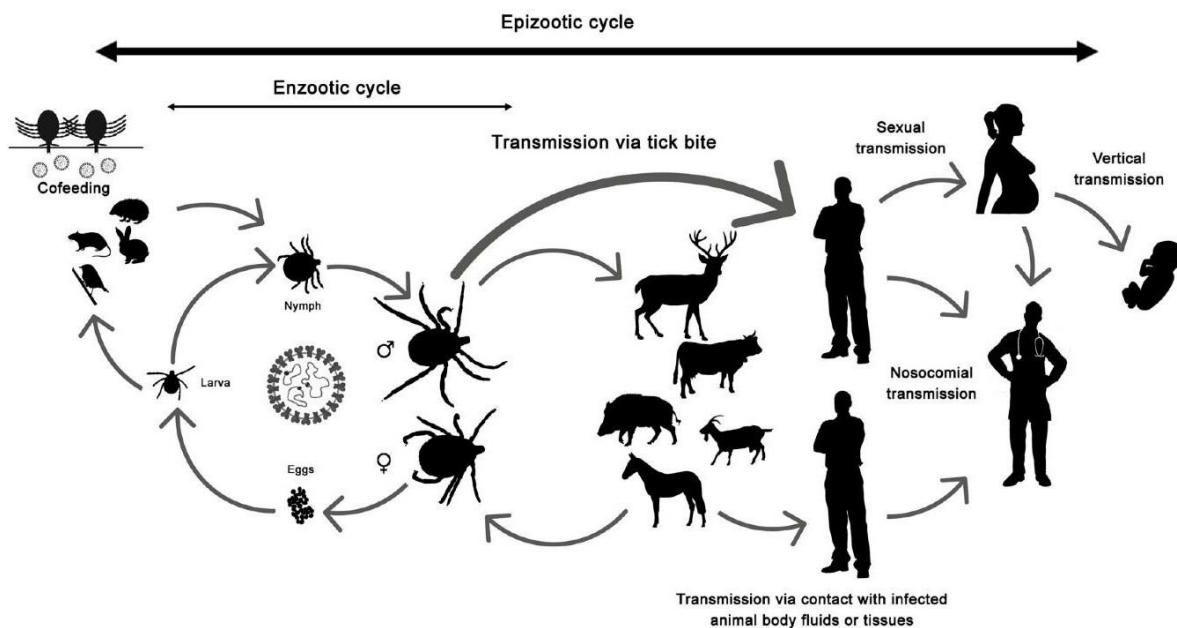


Figure 3. The natural epizootic cycle of CCHFV transmission, including an enzootic cycle, and transmission to humans through tick bite or via direct contact with infected body fluids of animals, and occasional human-to-human transmission [27].

The expanding geographical distribution of the main tick vectors due to climate change and through migratory birds, and the movement of livestock vertebrates as potential virus hosts are serious concerns for virus spread [28-30]. In correspondence with the geographical distribution of the virus, which overlaps with the expanding spatial spread of the principal tick vectors, CCHFV is a genetically diverse pathogen [7-10]. Three out of seven distinct lineages are circulating in Europe: the Europe-1 lineage (the most affected countries are Albania, Bulgaria, and Turkey), the Europe-2 lineage (isolated in Greece and Turkey), and the Africa-3 lineage (recently affecting the West-Mediterranean region, including Spain, Portugal and France) [28-38]. The spread of the Europe-2 lineage (including the Aigai virus – previously called as CCHFV AP92 strain – circulating in Greece and associated with less severe infections) is attributed to the *Rhipicephalus bursa* tick [32]. Due to global warming and the movement of migratory birds, the distribution of Mediterranean tick species has shifted further north in the previous decade [32-34].

CCHF cases have been reported from over 30 countries worldwide, with 10,000-15,000 infections per year, of which 500 were fatal [35]. The most affected countries are Albania,

Bulgaria, Georgia, Afghanistan, Kosovo, Russia, Spain, Portugal, Ukraine, Iraq, Pakistan, India, Turkey, Uganda and Sudan. Further serological evidence was found on potential virus circulation in Greece, Croatia, France, and Romania, as well. In Europe, approximately 6,000 CCHF cases were reported between 1953 and 2010. During this period, outbreaks were identified in Russia and Ukraine (including the Crimean Peninsula), Bulgaria, Albania, Kosovo, and Turkey [35, 36]. CCHF was first diagnosed in Bulgaria in the mid-1950s and became endemic in several regions of the country. In Greece, the first and so far only autochthonous case was reported in 2008, meanwhile the seroprevalence in specific regions of the county is over 5% [35]. In 2016, Spain reported its first autochthonous cases, and a retrospective study conducted in 2020 showed that another CCHF case had occurred in the same province in 2013 [37, 38]. Since 2016, 17 cases have been confirmed in three different regions of Spain, including one secondary nosocomial infection and 6 fatal cases [38]. Since 2002, Turkey reported over 16,500 confirmed cases, including 787 deaths. In North Macedonia, three cases were reported in 2023, one of which was fatal [35].

To detect the potential geographic spread and circulation of CCHFV, many seroepidemiological surveillance and local serosurvey studies have been performed and published worldwide [39, 40]. As the antibody prevalence in the general human and animal populations are good indicators for the presence or absence of the virus in a specific region, seroepidemiological studies are used to define risk areas of CCHFV circulation [40]. Furthermore, serological surveys in the animal populations are also the principal source of information to monitor areas with natural virus transmission and to identify exposed species [41]. Surveys among high-risk occupations for CCHFV infection, such as veterinarians, farmers, foresters, hunters and abattoir workers who are in close proximity to livestock or can acquire tick bite, also bear important predictive value [42].

Although there haven't been any confirmed human cases in Hungary so far, the principal vectors, *H. marginatum* and *H. rufipes* were identified multiple times and in various places in Hungary (Budapest, Veszprém, Pest, Somogy, Békés, Bács-Kiskun and Vas counties) between 2011 and 2021, and other potential tick vectors are also present in the country [20, 47-52]. Furthermore, local studies performed in Békés and Baranya counties between 2008 and 2013, focusing on rodents and brown hares (*Lepus europaeus*) showed seropositivity

among the animal population as well [53, 54]. Based on this data, in terms of the One Health approach, Hungary was categorized as a high evidence consensus country with no CCHF cases reported and no robust surveillance established. However, available data point toward the possibility of undetected CCHF cases and/or potential virus introduction to the country [55-57].

## 1.6. Diagnosis and treatment

According to the 18/1998. (VI. 3.) NM decree on the necessary epidemiological measures to prevent infectious diseases and epidemics, CCHFV diagnosis in Hungary is performed exclusively in the National Biosafety Laboratory (NBL), at the National Center for Public Health and Pharmacy (NCPHP), Budapest, under BSL-4 containment [58]. Work with appropriately inactivated samples (heating to 56°C for at least 30 minutes, gamma irradiation, or the addition of fixatives or disinfectants, including formalin, lysis buffer and absolute ethanol, sodium dodecyl sulfate, TRIzol or Triton-X100, etc.) can be performed in BSL-2 laboratory environment with precautions. Care should be taken when choosing an inactivation method to avoid interference with the diagnostic assay intended to be used. The diagnosis of human CCHFV infection must be confirmed by direct detection of virus nucleic acid or antigens, or by measurement of serological responses consistent with acute infection [21].

Viremia is the most common in the first few days after symptoms onset, but rapidly decreases after the first week. The primary method for diagnosis of CCHFV infection is nucleic acid detection by reverse-transcription polymerase chain reaction (RT-PCR) within the first two weeks after symptoms onset. Many different nucleic acid amplification tests (NAATs) have been published for the diagnosis of CCHFV infection including commercially available kits. Quantitative reverse-transcription polymerase chain reaction (RT-qPCR) targeting the conserved S segment is a commonly used and sensitive method in the first 10-12 days after symptom onset, and is generally more widely available than virus isolation. NAATs are performed from whole blood and serum samples, and saliva and/or urine samples are also suitable for follow-up testing. Quantification of the viral load may be useful for disease

prognosis, as viral loads among survivors tend to be lower than among cases with a fatal outcome and may correlate with symptom severity [59, 60].

*In vitro* virus isolation may be performed from samples taken within the first week of illness, in different cell lines with enhanced susceptibility (BHK-21, SW13, Vero, Vero E6, MDBK etc. cell lines) combined with either fluorescence focus or (pseudo)-plaque-based assays. *In vivo* virus isolation may be performed via intracerebral inoculation of suckling mice, or 4-6 weeks old mice deficient in type I interferon responses [21, 59, 60].

Serological testing is based on the detection of anti-CCHFV IgM antibodies or a 4-fold increase in anti-CCHFV IgG titers between serial serum samples. In the very early phase of the disease, the use of serological tests is less recommended, as specific antibodies can only be detected later, between days 5-14 after symptoms onset. Anti-CCHFV IgG antibodies are detectable for a maximum of 5 years in the serum of infected individuals [59-61].

Point of care rapid tests developed in recent years are currently being evaluated in endemic areas. Neutralizing antibody assays are not routinely used for CCHF diagnosis, however using cytopathic effect (CPE)-based pseudo-plaque or plaque reduction neutralization tests can be used for validation of other serological results [59-61]. Not only kits suitable for human diagnosis are available, but there are also novel assays for serological testing of animals, including cow and multi-species ELISA kits [62].

There is currently no licensed vaccine available against CCHFV infection. The only way of prevention is to protect against tick bites with repellents and to use appropriate protective clothing. Supportive therapy is used in the case of infection, but ribavirin has proven to be an effective antiviral agent in case of early administration [63].

## 2. Objectives

Due to the epidemic potential and the lack of sufficient countermeasures, the WHO identified CCHFV as one of the priority pathogens that pose great individual and public health risk [5]. Consequently, a Research and Development Blueprint was published to promote the development of diagnostics, therapeutics, vaccination and vector control strategies against CCHFV [5]. Such developments require standardized, well-characterized and reproducible laboratory protocols and models at the level of applied and fundamental research. Thus, by incorporating the international standards and requirements into our CCHFV research, we set out the following goals in my thesis:

1. Phenotypic and genetic characterization of the CCHFV Afg09-2990 laboratory strain in a stable and controlled cellular environment, in order to
  - i. describe virus growth kinetics in different cell lines;
  - ii. determine the optimal conditions for virus propagation in different cell lines for the purpose of downstream diagnostic development and application (multiplicity of infection, day to harvest, cell lines with high permissivity);
  - iii. determine the degree of growth-induced mutations in specific cell lines by revealing the phenotypic changes and genetic variations in the virus genome.
2. As part of the One Health concept, by using well-established and validated in-house and commercial serological assays, we aimed to perform the first broad-range CCHFV serological surveillance studies in Hungary among
  - i. the general human population (healthy blood donors); and
  - ii. free-range vertebrates as indicator animals (cattle and sheep).

### 3. Materials and methods

#### 3.1. Cell cultures

Four different cell lines susceptible for CCHFV were used in our experiments; Vero E6 (European Collection of Cell Cultures (ECACC), Porton Down, Salisbury, United Kingdom), Vero (NuvoNis Technologies GmbH, Vienna, Austria), and SW13 (ECACC) cells were maintained in the Dulbecco-modified Eagle medium (DMEM; VWR International bv, Leuven, Belgium) supplemented with 10% fetal bovine serum (FBS; Euroclone S.p.A., Pero, Italy) at 37°C under 5% CO<sub>2</sub>. BHK-21 (ECACC) cells were grown in Glasgow Minimum Essential Medium (GMEM; Biowest SAS, Rue de la Caille, France) supplemented with 10% FBS at 37°C under 5% CO<sub>2</sub>. In order to minimize bias introduction by the cell passaging and morphological changes, cells were passaged for a minimum of two and a maximum extent of 15 passages.

#### 3.2. Virus strain and propagation

The CCHFV Afg09-2990 strain (Genbank acc. No. HM452305.1, HM452306.1, HM452307.1) used in our experiments was provided by the Bernhard Nocht Institute for Tropical Medicine (Hamburg, Germany) through the European Virus Archive (EVA) [64]. The initial virus stock (passage 0; P0) was prepared from infected Vero E6 cell supernatant at the NBL, NCPHP under BSL-4 containment. The virus RNA copy number and tissue culture infectious dose 50% (TCID<sub>50</sub>) per mL of the initial virus stock were determined using RT-qPCR and infective titration as described later.

#### 3.3. Serial passaging and virus growth kinetics

Virus propagation was performed in 6-well plates (TPP Techno Plastic Products AG, Trasadingen, Switzerland). For the first passage (P1), suspensions of all four cell lines (at an initial 3,0E+05 cells/well density) were inoculated in three biological and three technical replicates by using three different multiplicity of infection values (MOI 0.005, 0.01 and 0.1). Supernatant of each sample was collected directly after inoculation (day post infection; dpi 0), then in every 24 hours until day 7 (dpi 0-7). Prior to titration, samples were stored at

– 80°C. Virus RNA copy number and TCID<sub>50</sub> per mL were calculated for each sample. Based on virus growth, the optimal MOI and dpi for harvesting the supernatant were determined and used for the subsequent passages (Appendix Figure 1). After the first passage, the virus was further propagated in the same cell lines for an additional four passages using the previously determined MOI and dpi for harvesting the supernatant (P2 - P5). Thereafter, the virus was further cross-passaged in every cell line for five additional times (P6 - P10). During the first cross-passage (P6), virus growth kinetics was assessed again. The optimal MOI and dpi were re-evaluated and used for subsequent passages accordingly (P7-P10). Virus RNA copy number and infective titer per mL were determined for each sample after every passage. During the first cross-passage (P6) and the final passage (P10) viral growth kinetics was also determined as described above.

#### 3.4. Nucleic acid extraction and RT-qPCR

Nucleic acid was extracted from 50 µL cell culture supernatant by adding 280 µL of AVL buffer (Qiagen, Hilden, Germany). After 10 minutes of incubation at room temperature, 280 µL ethanol (Szkarabeusz Laboratóriumi Kft., Pécs, Hungary) was added to each sample. Viral RNA was extracted using the Chemagic Viral DNA/RNA Kit special H96 (PerkinElmer, Waltham, Massachusetts, USA) on the Chemagic 360 Instrument (PerkinElmer, Waltham, Massachusetts, USA) running the Chemagic Viral300 360 H96 prefilling 18 min VD210204.che protocol. RT-qPCR was conducted on the LightCycler 480 Instrument II platform (Hoffmann-La Roche, Basel, Switzerland) using the LightCycler Multiplex RNA Virus Master kit (Hoffmann-La Roche, Basel, Switzerland). The applied primers and probes specific for the S segment (clade IV) were previously described by Sas *et al* [65].

#### 3.5. Infective titration

SW13 cells in DMEM with 10% FBS were seeded into 96-well plates (TPP Techno Plastic Products AG, Trasadingen, Switzerland) at a 10E+04 cells/well density. Cells were then inoculated in triplicates with the 10-fold serial dilutions of each sample. After incubating for 5 days at 37°C under 5% CO<sub>2</sub>, the supernatants were aspirated and cell monolayers were

inactivated and fixed with 4% formaldehyde solution. Fixated cells were stained by using crystal violet to observe cytopathic effect (CPE). Infective titers were calculated by the Spearman and Kärber method [66].

### 3.6. Whole genome sequencing (WGS)

Viral RNA extracted from the cell culture supernatants of P0, P1, P5, P6 and P10 samples were subjected to DNase I digestion (Turbo DNase; Invitrogen, Thermo Fisher Scientific, Waltham, Massachusetts, USA) followed by AMPure XP bead (Beckman Coulter, Brea, California, USA) purification performed according to manufacturer's instructions and eluted in 10 µL nuclease-free water. To avoid primer bias, randomly amplified DNA products were prepared from the purified RNA samples of all three biological replicates by using the single-primer sequence-independent amplification (SISPA) protocol and K/K8N primers as previously described [67]. After the enrichment, parallel samples were pooled together for the Illumina Nextera XT V2 library preparation (Illumina, Waltham, Massachusetts, USA) and sequenced on the Illumina MiSeq instrument (Illumina, Waltham, Massachusetts, USA) using 2 x 150 bp paired-end chemistry (Reagent Kit v2 Micro; Illumina, Waltham, Massachusetts, USA).

### 3.7. Sample selection for the human serosurveillance

As part of the retrospective human serosurveillance, serum samples ( $n = 2700$ ) kindly provided by the Hungarian Blood Transfusion Service were screened for anti-CCHFV IgG antibodies. Randomly selected volunteer blood donors aged between 18–65 years were enrolled from all 20 NUTS3 regions (Nomenclature of Territorial Units for Statistics) of Hungary. Sample size was fitted to the Hungarian demographic data registered by the Hungarian Central Statistical Office, taking the region of residency, age, and gender distribution into consideration to reach 0.04% prevalence of the population (KSH data, 2018) [68]. Only registered Hungarian citizens were enrolled. Serum samples were taken during the regular blood donation process between 2008 and 2017. Obtained data (date of birth, gender, residence, and history of previous infectious diseases) were anonymized before blood

donation; however, no information about travel history was available. Samples were stored at -20°C before serological testing.

### 3.8. Sample selection for the animal serosurveillance

To perform the first broad-range animal serosurveillance in Hungary, blood specimens were collected from healthy free-range animals (cattle and sheep) as part of monitoring programs for various animal diseases in 2017. The samples were tested by the Laboratory of Immunology of the Veterinary Diagnostic Directorate, National Food Chain Safety Office (Budapest, Hungary). Subsequently, archived specimens were made available to the NBL, NCPHP by the National Food Chain Safety Office. In total, 1905 serum specimens were tested for the presence of anti-CCHFV IgG antibodies, comprising 1391 serum samples obtained from cattle and 514 samples from sheep.

### 3.9. Serological testing

#### 3.9.1. Screening the human serum samples

All serum samples obtained from healthy blood donors were screened for anti-CCHFV-specific IgG antibodies by using in-house IIFA detecting all CCHFV-specific antibodies including polyclonal immune response. The immunofluorescence slides were produced at the NBL, NCPHP under BSL-4 containment, using the CCHFV Afg09-2990 strain to inoculate Vero E6 cells. During the validation process, the immunofluorescence slides were tested to reveal potential cross-reactions with human IgG and IgM antibody positive samples of previously confirmed patients for tick-borne encephalitis virus, Hantavirus, *Coxiella burnetii*, *Leptospira sp.*, *Francisella sp.*, *Mycoplasma sp.*, Epstein-Barr virus, and Cytomegalovirus.

During the first screening, heat inactivated (56°C for 30 minutes) sera were diluted at 1:20 in phosphate-buffered saline (PBS), and reactive samples were further titrated to determine the final antibody titer. Diluted serum samples were added to the IIFA slides, and incubated for 1 h at 37°C. After incubation, slides were washed three times in PBS+Tween 20 (PBST) and stained with Anti-Human IgG (whole molecule) –FITC antibody secondary antibody

(Merck KGaA, Darmstadt, Germany) diluted at 1:50. Slides were incubated for 30 min at 37°C. After washing three times in PBST, slides were air-dried and mounted with glycerin and covered with glass. For the positive control, anti-CCHFV IgG-positive polyclonal mouse serum was used in 1:160 dilution.

Fluorescence read-out was performed with the Leica DMi8 (Leica Microsystems, Wetzlar, Germany) microscope system. Images were processed with the LAS X Life Science Microscope Software (Leica Microsystems, Wetzlar, Germany) software. Fluorescence was evaluated for anti-CCHFV IgG-specific staining compared to the positive control by two independent individuals.

IIFA-positive results were verified by using a commercially available recombinant nucleoprotein (rNP) ELISA kit (VectorBEST, Novosibirsk, Russia). For the ELISA, a sample dilution of 1:100 was used and processed according to the manufacturer's instructions. Reactive samples were also screened for serological IgG reactivity against Hantavirus, West Nile virus, tick-borne encephalitis virus, and IgM reactivity against Epstein-Barr virus and Cytomegalovirus, to exclude non-specific reactions.

### 3.9.2. Screening the animal serum samples

Serum specimens obtained from cattle and sheep were inactivated (56°C for 30 minutes) and centrifuged at 7000×g. The sera of animals from the same geolocation were combined into pools of a maximum of five samples.

To screen the cattle, the Cow Crimean-Congo Hemorrhagic Fever Virus IgG (CCHF-IgG) ELISA Kit (Abbexa Ltd., Cambridge, United Kingdom) was used according to the manufacturer's instructions in 1:5 sample dilution. Samples of the positive or equivocal pools were tested further individually with the same ELISA kit (in two-fold dilution) and two types of immunofluorescent assays. The IIFA slides were produced and validated as described above (see Section 3.9.1.). Samples and sample pools were diluted in 1:20 in PBS, added to IIFA slides, and incubated for 1 h at 37°C. After incubation, slides were washed three times in PBST and stained with the FITC-conjugated Anti-Bovine IgG (whole molecule) secondary antibody (Merck KGaA, Darmstadt, Germany) diluted 1:300. Slides were incubated for 30 min at 37°C. For the EUROIMMUN CCHFV Mosaic 2 IgG immunofluorescence assay

(EUROIMMUN Medizinische Labordiagnostika AG, Lübeck, Germany), which contains transfected Vero cells expressing the CCHFV NP and GPC antigens, samples were diluted 1:20. The slides were stained with the FITC-conjugated Anti-Bovine IgG (whole molecule) secondary antibody at the dilution 1:300. Otherwise, the EUROIMMUN assay was performed according to the manufacturer's instructions. Read-out of the IIFA slides was performed as detailed above (see Section 3.9.1).

To investigate the sheep serum pools, samples were pooled and diluted 1:20 in PBS for the in-house IIFA screening. Reactive pools were then tested further individually at the dilution 1:20 with two immunofluorescent assays. The in-house and the EUROIMMUN CCHFV Mosaic 2 IgG IIF assays were performed as described above, and slides were stained with the FITC-conjugated Anti-Sheep IgG (whole molecule) secondary antibody (Merck KGaA, Darmstadt, Germany) at the dilution 1:400.

End-point serum titration of the individual positive samples was performed in a two-fold serial dilution (dilution range 1:10–1:640) using the in-house IIFA. Among the cattle samples, those that showed reactive results in ELISA and both IIFA assays were considered positive, and among the sheep samples, positivity was concluded if reactivity was detected in both the in-house and the commercial IIFA.

### 3.10. Data analysis

#### 3.10.1. Virus growth kinetics

Virus growth kinetics during the first passage (P1), the first cross-passage (P6) and the final passage (P10) was determined by the mean virus RNA copy number per mL and geometric mean TCID<sub>50</sub> per mL of the replicates at each sampling time point (dpi 0 – 7). Kinetic curves (x: days post inoculation, y: virus titer) and standard deviations (SD) were visualized using the GraphPad Prism 9.5.0 software (GraphPad Software Inc., Boston, MA, USA).

To analyze the effect of the different cell lines, the MOI and the passage number on the log virus growth during P1, P6 and P10, and an ordinary two-way analysis of variance (ANOVA) was performed within the GraphPad Prism 9.5.0 software. Reported P values are significant at the 5% level. Cell susceptibility – described as the initial (d0) virus RNA copy number

used for inoculation over the generation of 1 TCID<sub>50</sub> per mL – was also determined during P1, P6 and P10.

### 3.10.2. Whole genome analysis and variant call

For the genome analysis, forward and reverse sequencing reads in fastq files were quality trimmed by TrimGalore and mapped to reference S (Accession No: HM452305.1), M (accession No: HM452306.1), and L (accession No: HM452307.1) segments using bowtie2 and SAMtools. Variants were called in cDNA sequences. High-frequency variants occurring at a rate equal to or above 10% of all reads were called in the regions that met the minimum sequencing depth criteria set at 100. Distribution of nucleotide variants by segment and genome position for each sample was determined using R and the Geneious Prime 2021.2.2 software (Biomatters, Auckland, New Zealand). Average variant frequency (VF) and the number of single nucleotide polymorphisms (SNPs) were determined for each sample and visualized using the GraphPad Prism 9.5.0 software. Analysis of the nucleotide variants and manual annotation of high-frequency mutations over 40% frequency (consensus level) were performed and compared to the whole genome sequence of the P0 inoculum virus stock.

### 3.10.3. Descriptive analysis and geographical distribution: human serosurveillance

For the descriptive analysis, the number of reactive samples and seroprevalence (defined as the percentage of identified anti-CCHFV IgG-positive samples in the study groups and 95% confidence intervals [CI]) were determined for each NUTS3 region, age, and gender group by using the SPSS Statistics v17.0 software (SPSS Inc., Chicago, USA). To describe the geographical distribution of seroprevalence, results were visualized at the NUTS3 level using the EMMA tool (ECDC European Map Maker) [69]. The location of blood donation and residency of seropositive donors were also assessed and visualized.

### 3.10.4. Descriptive analysis and geographical distribution: animal serosurveillance

Prevalence was defined as the percentage of anti-CCHFV IgG-positive samples in the study groups with 95% CIs in each NUTS3 region and district using GraphPad Prism 9.5.0

software. To describe the geographical distribution of seropositive animals at the district level, results were visualized by Quantum GIS 3.0 software (ESRI Inc., Redlands, California, USA) with district administrative borders obtained via the OpenStreetMap database [70].

## 4. Results

### 4.1. *In vitro* growth-induced adaptation to cell lines

#### 4.1.1. MOI-dependent virus growth kinetics

During the first passage of the CCHFV Afg09-2990, we determined the MOI-dependent virus growth kinetics in Vero E6, Vero, SW13 and BHK-21 cell lines (Figure 4). CPE caused by virus replication was detected only in SW13 cells. When comparing the cell lines, the highest virus RNA copy number per mL was determined in SW13 at all three MOIs (Appendix Table 1). Virus growth kinetics showed similar trends in BHK-21 cells as in SW13 (Figure 4A-C), however, without producing CPE in the cells. Similar kinetics were seen in Vero and Vero E6 cells with an average of 0.457 log higher virus copy number per mL in Vero cells at all MOIs (Figure 4A-C, Appendix Table 1). According to our results, the maximum virus RNA copy number per mL increased to the same extent at all MOIs, but depended on the cell line (Figure 4A-C). Consequently, the logarithmic increase in virus RNA copy number per mL was higher when inoculated at MOI 0.005 compared to the higher MOIs. According to the ordinary two-way ANOVA, the MOI and the cell line factors had significant effect on the logarithmic increase in virus RNA copy number ( $P < 0.0001$  and  $P = 0.0319$ , respectively).

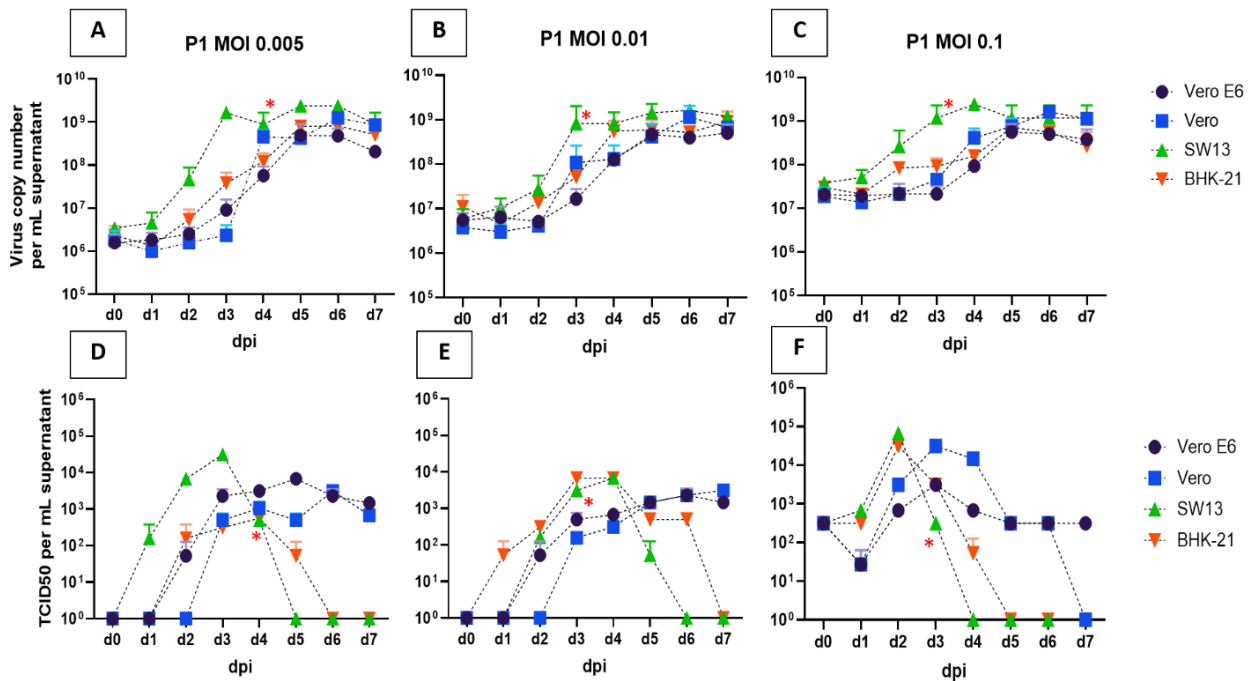


Figure 4. Virus growth kinetics during P1 at three different MOIs. A-C. Kinetic curves on the virus RNA copy number per mL at the three MOIs examined during this study (MOI 0.005 (A), 0.01 (B) and 0.1(C)). D-E. Kinetic curves on the TCID50 per mL supernatant at the three MOIs (MOI 0.005 (D), 0.01 (E), 0.1 (F)). The four cell lines are indicated with different colors: Vero E6 (dark blue), Vero (blue), SW13 (green), BHK-21 (orange). Dpi: day post infection. Standard deviation (SD)/geometric SD is visualized by error bars. Full cytopathic effect (CPE) in SW13 cells is indicated with red \* on the respective dpi in the graph.

When comparing the infective titers (Appendix Table 1), the highest TCID50 per mL was measured when passaged in SW13 cells (Figure 1D-F), which started to decline rapidly after producing CPE. The logarithmic increase in the infective titer was the highest at MOI 0.005 in all cell lines, however it was reached on a later day post infection (dpi) compared to MOI 0.1 (48h later on average, Appendix Table 1). Interestingly, the cell line factor had no effect on the logarithmic increase in the infective titer ( $P = 0.2818$ ), while the MOI affected it significantly ( $P < 0.0001$ ).

We also compared how the dpi with the highest infective titers depended on the MOI (Appendix Table 1). Both the MOI and the cell line showed significant effect ( $P = 0.0039$

and  $P = 0.0122$ , respectively). Based on the results of the MOI-dependent virus growth kinetics, we chose MOI 0.005 for the subsequent (P2-P10) passages for all cell lines and dpi 5 (Vero E6), 6 (Vero), 3 (SW13) and 4 (BHK-21) for harvesting the supernatant of the subsequent four (P2-P5) passages.

#### 4.1.2. Effect of serial passaging and cell line on the virus growth and permissivity

After the first cross-passaging (P6), the dpi with the highest infective titers were assessed again (Appendix Table 2), and the subsequent cross-passages and harvesting the supernatant were performed accordingly. No clear trend was observed in the maximum virus RNA copy number per mL, when compared during P1, P6, and P10, however deviation decreased among cell lines (Appendix Table 2). Based on the ANOVA, the cell line factor affected the logarithmic increase of virus RNA copy number per mL significantly ( $P < 0.0038$ ), when comparing P1, P6 and P10 passages on the same cell lines (without cross-passaging).

In the case of the infective titers, there was no clear trend between P1, P6 and P10, however slightly higher infective titers with larger overall deviation between cell lines were observed during P10 compared to P6 (Appendix Table 2). The overall highest infective titer was obtained in Vero cells during P10 ( $4.38E+03 - 2.72E+05$  TCID<sub>50</sub> per mL) on dpi 2-4, depending on the cell line. The highest deviation in the infective titers was observed when the virus was cross-passaged from Vero E6 cells to other cell lines.

Permissivity of cell lines for CCHFV (determined as the ratio of the initial virus RNA copy number per mL over the generation of 1 TCID<sub>50</sub> per mL) was calculated and compared during P1, P6 and P10 (Figure 5) [73]. According to our results, the highest initial permissivity (at P1) was found in SW13 cells ( $1.09E+02$  copies/TCID<sub>50</sub>), however that reduced by 0.81 log by P10 (Figure 5C). The highest increase in permissivity (1.99 log on average) between P1 and P10 was seen when the virus was passaged in Vero cells, suggesting adaptation to Vero cells after cross-passaging from other cell lines (Figure 5B). For Vero E6, we obtained a slightly lower initial permissivity compared to SW13 ( $2.31E+02$  copies/TCID<sub>50</sub>, respectively), and serial passaging did not result in enhanced permissivity over time (Figure 5A). The lowest initial permissivity was observed in BHK-21 ( $5.16E+03$

copies/TCID50), however it increased with 1.30 log on average due to serial passaging (Figure 5D).

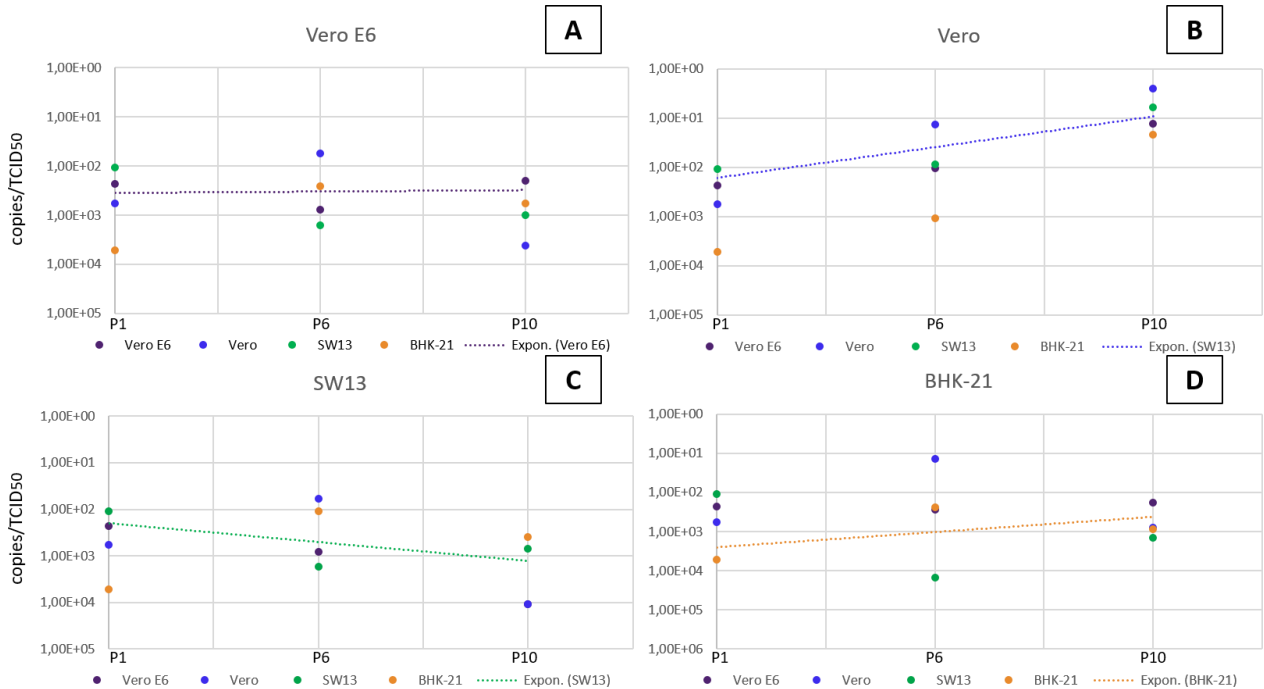


Figure 5. Permissivity of the cell lines for CCHFV. Graphs are shown by new cell lines after cross-passaging. Original cell lines are indicated with colors (Vero E6: dark blue, Vero: blue, SW13: green, BHK-21: orange). P1: passage 1. P6: passage 6. P10: passage 10. Baseline permissivity (control cells lacking cross-propagation) is indicated with dashed trend line. y-axis (labeled as copies/TCID50) representing cell permissivity for CCHFV is visualized in reverse. Thereby, increasing permissivity is characterized by a curve with a positive slope.

#### 4.1.3. Growth-induced variant distribution in the viral genome

The overall average genome coverage with sequencing depth over 100x was 99.55% (91.95% - 100%) in the coding regions. During the study, we identified an overall number of 953 SNPs, including 256 unique mutations with frequency over 10%. The average variant frequency (VF) based on all samples was 16.35% (95% CI 11.66 – 21.04%), 15.53% (95% CI 12.87 – 18.18%) and 33.74% (95% CI 27.43 – 40.04%) in the S, M and L segments, respectively.

In the S segment, the average VF increased from 11.12% (P1) to 19.61% (P10) (Figure 6A-D). In the M segment, the average VF was 13.93% (P1), and increased to 16.27% (in the range of 13.20% in SW13 and 19.17% in BHK-21, Figure 6E-H) by P10, significantly depending on the new cell line ( $P = 0.0301$ ). In the L segment, the average VF showed strong increase (from 16.27% (P1) to 39.23% (P10),  $P < 0.0001$ ) during serial passaging (Figure 6I-L). The number of SNPs with frequency over 10% was 1.2, 1.77 and 1.13 per kb in the S, M and L segments, respectively.

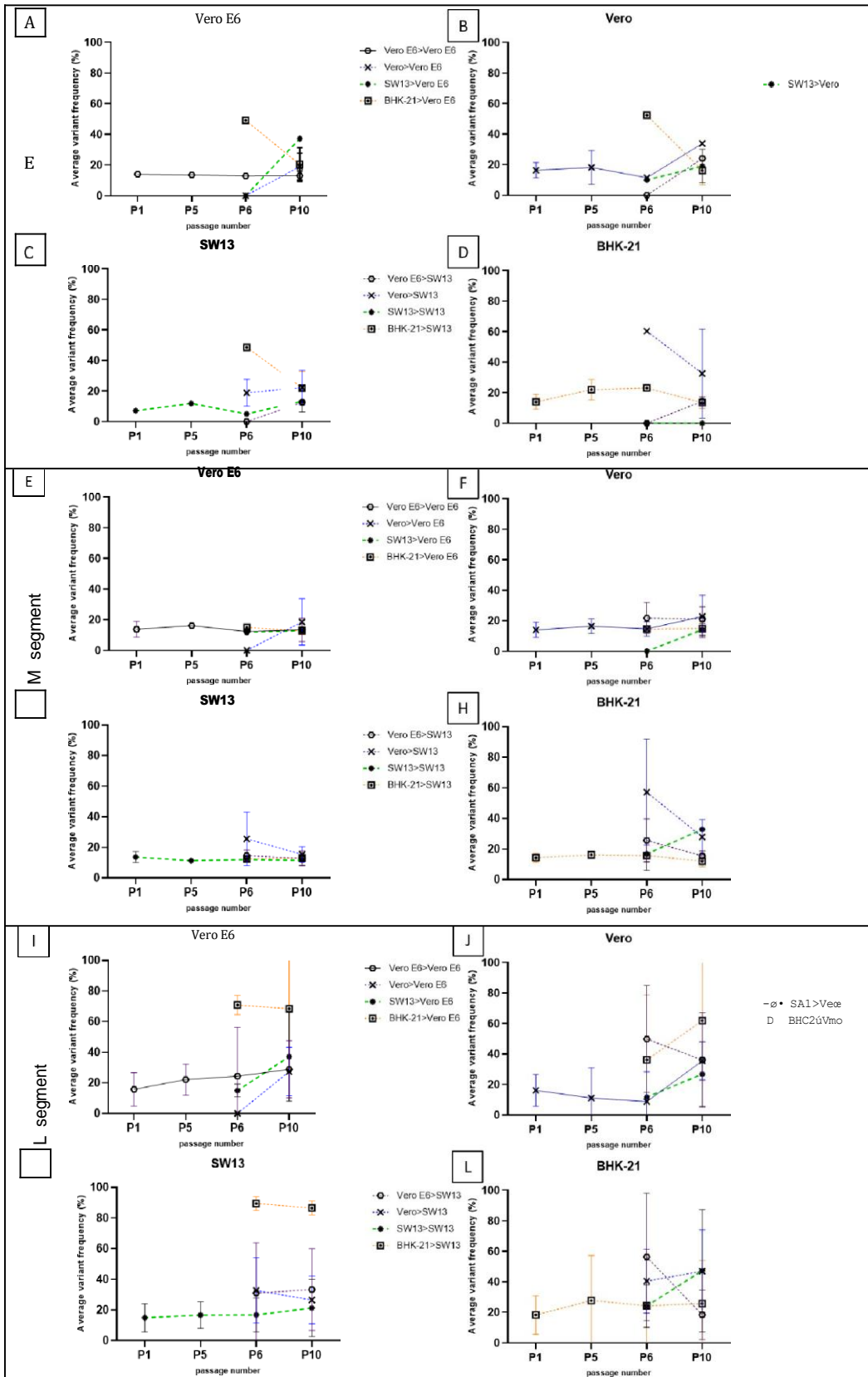


Figure 6. Average variant frequency by genome segments and by cell lines used for propagation. New cell lines after cross-passaging are shown in separate graphs (A-L), previous (original) cell lines are highlighted in colors. Data is shown for each passage (P1, P5, P6, P10). Error bars represent standard deviation (SD).

We also determined the distribution of all identified nucleotide variants over 10% frequency along the genome segments by genome position for each sample (Figure 7). Variants within the P0 inoculum CCHFV stock were also examined in order to set the genetic baseline and track the evolution of the subclonal diversity of the virus, but were excluded from the visualization.

In the S segment (Figure 7A), we found two individual nt variations with frequencies over 40% (highlighted with red arrows). Both variations emerged when the virus was cross-passaged from BHK-21, and when passaged from Vero to BHK-21. Despite that the average VF did not show strong cell-specificity in this segment ( $P = 0.167$ , Figure 6A-D), the number of mutations increased (with 0 – 2.5 nt variations per kb, depending on the cell line) during serial passaging, especially when passaged in Vero E6 and SW13 (Figure 6A and 6C, Figure 7A). In the M segment (Figure 6E-H), a constant average VF was found during serial passaging, independent of the passage number ( $P = 0.0556$ ), however it was affected by new cell lines ( $P = 0.0301$ ). Interestingly, the number of individual SNPs was higher during P1 for all cell lines compared to subsequent passages (see Figure 7B, first column green dots). During P10, an increase in the number of nt variations was also observed, compared to previous passages (Figure 7B, purple dots). Interestingly, most SNPs with frequency over 40% emerged when the virus was previously passaged in Vero cells (Figure 4B row 3, high frequency SNPs highlighted with red arrays). In the L segment (Figure 6I-L), VF increased significantly by P10, compared to P1 ( $P < 0.0001$ ), in addition to the high number of SNPs seen during the first passage (Figure 7C, green dots, 35 – 41 nt variations, depending on the cell line), which decreased during the subsequent passages. This indicates the rapid emergence of low-frequency quasi-species during P1, and positive selection and fixation of certain consensus-level mutations in the L segment due to serial passaging and possible adaptation to the cell lines.

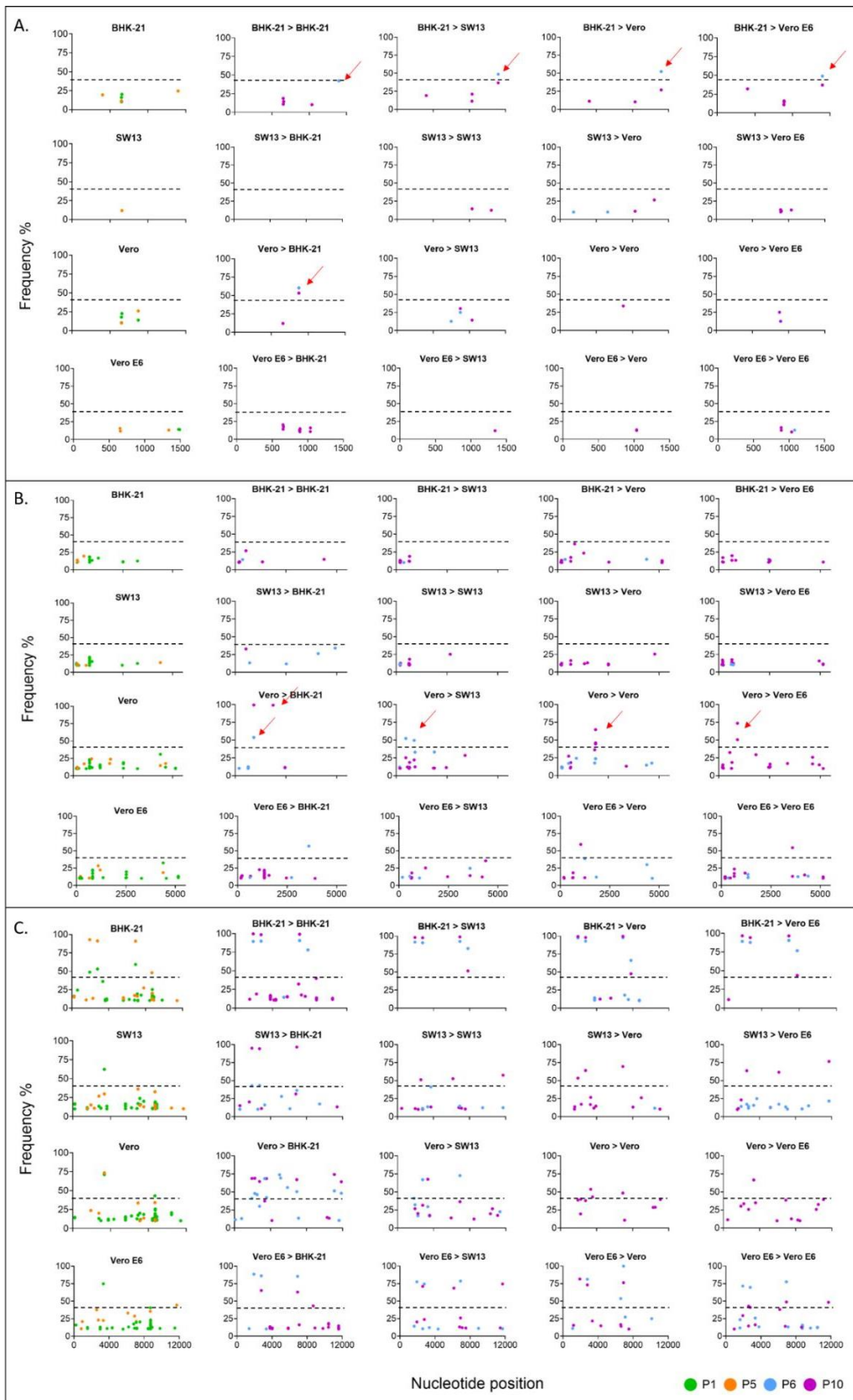


Figure 7. Distribution of all identified variants with rounded frequency over 10% along the whole genome of the CCHFV for the P1, P5, P6 and P10 samples (A. S segment, B. M segment, C. L segment). First column shows the P1 (green) and P5 (orange) passage results by cell line. Columns 2-5 represent P6 (blue) and P10 (purple) cross-passages indicated as original cell line>new cell line. Mutations of particular interest emerging with frequency over 40% (indicated by a dashed line) are highlighted with red arrows.

#### 4.1.4. Analysis of nucleotide change preferences

Nucleotide change preference among variants over 10% was also determined in all three genome segments compared to the nt variants identified in the P0 inoculum stock genome (Appendix Figure 2). In the inoculum stock (previously amplified in Vero E6 cells), an overall number of 18 high-frequency SNPs were identified compared to the reference sequence of the CCHFV Afg09-2990 strain; including 4 (G>A, T>C and C>T) variations in the S segment, 4 (A>G, G>A, T>A) in the M segment, and 10 mutations (A>G, A>T, C>T, T>A and T>C) in the L segment.

When further passaged, the most common high-frequency nt change in the S segment was T>C for all cell lines (42.11% (95%CI: 32.64 – 51.57%). A>C nt change occurred specifically when passaged to Vero E6 cells (18.42%, 95%CI 8.96 – 27.88%), and T>G nt change was mostly identified when passaged in BHK-21 cells (15.79%, 95%CI 6.33 – 25.25%).

In the M segment, the most common nt changes were A>C and A>G with 24.76% (95%CI: 20.21 – 29.32%) and 20.95% (95%CI: 16.40 – 25.51%) frequency of occurrence, respectively, for all cell lines. Interestingly, C>A change was more abundant in the viral genome when passaged in Vero E6 and SW13 cells.

No high abundance cell line-specific nucleotide change preferences were seen in the L segment; the most common SNPs were T>C with 26.33% (95%CI: 21.69 – 30.96%) and A>G with a 23.18% (95%CI: 18.55 – 27.82%) frequency of occurrence. Interestingly, C>A nt change occurred only when the virus was passaged in SW13 cells (1.38%, 95%CI 0 – 6.01%), whereas C>G (3.73%) and T>G (8.25%) nt variations showed BHK-21 specificity.

#### 4.1.5. Annotation of consensus level mutations

Annotation of the nucleotide variants with frequency over 40% was performed and compared to the consensus sequence of the P0 inoculum virus stock (Table 1). We found two SNPs in the S segment, of which one mutation is a probable consequence of adaptation to the BHK-21 cell line (see also Figure 7A). The silent mutation I448I (nt 1399, ATT>ACT) was present in the P0 virus genome with 3.65% frequency, and emerged when passaged in the BHK-21 cells to 26.51% by P5. After cross-passaging in Vero E6, Vero and SW13, the average frequency was 42.4 – 52.4% during P6, depending on the cell line, and the mutation persisted through P10 (VF was between 26.9 – 37.2%, depending on the cell line, see Figure 7A row 1).

In the M segment we found no variations with frequency over 40% during the first five serial passaging (Figure 7B, column 1). After cross-passaging, the probability of adaptation to specific cell lines arose in the case of three mutations (out of 6 unique SNPs). Silent mutation L276L (nt 920, TTA>TTG) in the GP38 region of the M segment emerged Vero cell-specifically to 24.3% by P5, and persisted further in the Vero (50.3%), Vero E6 (53.47%) and BHK-21 (99.5%) cells by P10. The mutation showed slow reversion in SW13 cells decreasing to a 12.4% frequency by P10. Mutation E594K (nt 1872, GAG>AAG) in the Gn coding region emerged when the virus was passaged in Vero cells (P5: 23.80%) and it emerged in Vero E6 (46.0%), Vero (44.5%) and BHK-21 (64.7%) cells, but reverted in SW13 cells (33.3% by P6 and 10.6% by P10). Mutation D1168G (nt 3595, GAC>GGC) in the Gc region emerged when the virus was passaged in Vero E6 cell line, and persisted with a frequency around 10% when serially passaged in Vero E6, SW13 and BHK-21. The mutation emerged with higher frequency (54.5%) by P10 when passaged in Vero cells. Other high-frequency mutations identified in the M segment showed no cell-line specificity, but there were mainly A>G, G>A, T>A and C>T nucleotide changes.

In the L segment, an overall number of 16 individual SNPs with over 40% frequency occurred. Among them 10 mutations can be linked specifically to a cell line. Two nt variations were present in the original P0 sequence as ambiguities; the A2279V (nt 6913, GTA>GCA) mutation in the RdRp region with a frequency of 77.11%, that further persisted

in all cell lines with 12.06 – 100.0% frequency depending on the cell line. A2279V emerged with high VF when passaged from or to BHK-21 cells (over 90.0%), but showed reversion when passaged to SW13. Silent mutation E1093E (nt 3352, GAG>GAA) with a 42.17% frequency in the P0 genome persisted further with high frequency (over 53.0%) when the virus was passaged in Vero cells. E1093E showed complete reversion in BHK-21 cells. Mutation D618E (nt 1931, GAT>GAA) in the zinc-finger domain also emerged when passaged in all cell lines after P1, and persisted throughout the long-term passaging, but with higher frequency when passaged in BHK-21 (over 90% frequency) compared to the other cell lines. Similar to the D618E mutation, P899P (nt 2774, CCT>CCC) in the NP-binding region, and F2576F (nt 7805, TTT>TTC) in the RdRp motif emerged with high frequency when the virus was passaged in BHK-21 cells, and persisted further in all cell lines. Besides E1093E, two further SNPs were identified that emerged exclusively when the virus was passaged in Vero cells (A1159T and T3667A), and fixed in the viral genome and persisted after cross-passaging to other cell lines. In the L segment, three additional SNPs emerged specific to Vero E6 and SW13 cell lines. Silent mutation N2025N (nt 6152, GAC>GAT) persisted only in Vero E6 and SW13 cells with a frequency of 38.20 – 68.60%. Mutations A3879V (nt 11713, GCA>GTA) and R837S (nt 2588, AGA>AGT) both emerged in the NP-binding site as quasi-species Vero E6 and SW13-specifically, and persisted by P10 in all cell lines with over 40% VF.

Table 1. Annotation of the nucleotide variants with frequency over 40%. aa: amino acid, nt: nucleotide.

aa change	nt position	average depth of coverage	nt change	type	genome region	relevance/behaviour
<b>S segment</b>						
I448I	1399	2855	ATT>ACT	silent	NP head domain	Quasi-species emerged in BHK-21 cells; mutation fixed in the viral genome and persists when passaged in other cell lines.
<b>M segment</b>						
L276L	920	12041	TTA>TTG	silent	GP38	Quasi-species emerged in Vero cells; mutation fixed in the viral genome and persists when passaged in other cell lines. Slow reversion in SW13 cells.
E594K	1872	9260	GAG>AAG	non-silent	Gn	Quasi-species emerged in Vero cells, and adapted to Vero E6, Vero and BHK-21 cells. Slow reversion in SW13 cells.
D1168G	3595	2515	GAC>GGC	non-silent	Gc	Low-frequency quasi-species emerged in Vero E6, and persisted in Vero E6, BHK-21 and SW13 with low frequency, and in Vero cells with high frequency.
<b>L segment</b>						
D618E	1931	3282	GTA>GCA	non-silent	zinc-finger (ZF) domain	Potential NP-binding function alteration; BHK-21-specific virus adaptation,

						persisting as quasi-species in the other cell lines.
R837S	2588	10902	AGA>AGT	non-silent	NP-binding site	Vero E6 and SW13-specific virus adaptation.
P889P	2774	6422	CCT>CCC	silent	NP-binding site	BHK-21-specific virus adaptation, persisting as quasi-species in the other cell lines.
E1093E	3352	7137	GAA>GAG	silent		Present in P0 genome; emerged Vero cell specifically, reverted in BHK-21 cells.
A1159T	3552	6839	GCA>ACA	non-silent		Vero cell-specific persisting quasi-species, but reverts in other cell lines.
N2025N	6152	3103	GAC>GAT	silent		Vero E6 and SW13-specific virus adaptation.
A2279V	6913	5191	GCA>GTA	non-silent	RdRp motif	Potential catalytic activity alteration; present in P0 genome; emerged in all cell lines as quasi-species but strong adaptation to BHK-21. Reverts in SW13 cells.
F2576F	7805	8832	TTT>TTC	silent	RdRp motif	BHK-21-specific nt variation.
T3667A	11076	52363	ACC>GCC	non-silent	NP-binding site	Vero-specific nt variation.

A3879V	11713	63847	GCA>GTA	non-silent	NP-binding site	Vero E6 and SW13-specific nt variation.
--------	-------	-------	---------	------------	-----------------	---

## 4.2. Human serosurveillance

### 4.2.1. Study population, sample selection, and data collection

A total of 2700 samples were received from 73 municipalities within all 20 NUTS3 regions of Hungary. Donors were categorized into three age groups (18–34, 35–50, and 51–65 years), and the sample size was fitted to correspond to the Hungarian demographic data. Group I (18–34 years) comprised 902 donors (33.41%); Group II (35–50 years) comprised 904 donors (34.48%); and Group III (51–65 years) comprised 894 donors (33.11%). Overall, 1463 male (54.19%) and 1237 female (45.81%) donors were tested. Due to the low number of female blood donors aged between 51 and 65 years, male donors were overrepresented in Group III (18.81%) when compared with the Hungarian population as a whole (14.19%).

### 4.2.2. Serological screening

Altogether, 12 samples (0.44% seroprevalence; 95% CI, 0.19–0.69%) were positive for anti-CCHFV IgG antibodies by IIFA (Table 2). The mean age of blood donors with reactive results was 37 years (range, 22–64 years). Two samples showed high IgG positivity up to a dilution of 1:160, five were positive at a final dilution of 1:80, and five were positive at a final titer of 1:40. To confirm the IIFA results, reactive samples were also tested using a commercially available rNP ELISA kit. The ELISA results were concordant with the IIFA results for eight samples (IIFA titers of 1:160 and 1:80) and two borderline samples (IIFA titers of 1:80 and 1:40), but were discordant (negative) for two IIFA-reactive samples with an antibody titer of 1:40 (OD values not shown). Anti-CCHFV IgG-positive samples showed no cross-reactivity with Hantavirus, West Nile virus, tick-borne encephalitis virus, or *Leptospira sp.* IgG antibodies, or with Epstein–Barr virus and Cytomegalovirus IgM antibodies in the confirmatory ELISA and IIFA testing.

Table 2. Seropositive donors identified during the study [71].

<b>Gender</b> F: female M: male	<b>Age</b>	<b>NUTS3 region</b>	<b>Place of donation</b>	<b>Residency of the donor</b>	<b>IIFA titers</b>	<b>rNP ELISA</b>
M	22	Bács- Kiskun	Kecskemét	Kecskemét	1:160	Positive
M	31	Jász- Nagykun- Szolnok	Szolnok	Szolnok	1:160	Positive
F	26	Győr- Moson- Sopron	Sopron	Győr	1:80	Positive
F	43	Veszprém	Veszprém	Hajmáskér	1:80	Positive
M	25	Budapest	Budapest	Budapest	1:80	Positive
M	33	Fejér	Székesfehérvár	Nagyvenyim	1:80	Positive
M	38	Jász- Nagykun- Szolnok	Szolnok	Tiszanoka	1:80	Borderline
M	39	Vas	Répcelak	Répcelak	1:40	Positive
M	25	Vas	Répcelak	Nick	1:40	Positive
M	64	Somogy	Siófok	Balatonszemes	1:40	Borderline
M	60	Győr- Moson- Sopron	Sopron	Győr	1:40	Negative
F	33	Jász- Nagykun- Szolnok	Szolnok	Szolnok	1:40	Negative

#### 4.2.3. Descriptive analysis

Among the ten positive samples detected by both assays (0.37%; 95% CI, 0.14–0.6%), eight were from male donors (80.0%) and two were from female donors (20.0%). The calculated seroprevalence was 0.55% (95% CI, 0.17–0.93%) among male donors and 0.16% (95% CI, 0–0.38%) among female donors. The mean age of positive male donors was 34.6 years (range, 22–64 years), whereas that of female donors was 34.5 years (range, 26–43 years). When comparing the different age groups, seven donors belonged to Group I, two to Group II, and one to Group III. The most affected age group was Group I, with a calculated seroprevalence of 0.78% (95% CI, 0.21–1.35%). Seroprevalence in Groups II and III was 0.22% (95% CI, 0–0.53%) and 0.11% (95% CI, 0–0.33%), respectively. The highest prevalence (1.04%; 95% CI, 0.13–1.95%) was observed among male donors in Group 1. No seropositivity was identified among female donors aged between 51 and 65 years (Group III).

#### 4.2.4. Geographical distribution

Serum samples were received from all 20 NUTS3 regions of Hungary (Appendix Table 3). Positive samples were identified in 8 NUTS3 regions, with a prevalence of between 0.20% and 2.97% (with mean prevalence of 1.38%). The highest seroprevalence was observed in Jász-Nagykun-Szolnok county in central Hungary (the Great Plain), with two confirmed samples and one probable sample (2.97%; 95% CI, 0–5.71%). The western and central parts of the Transdanubian region were also affected (Győr-Moson-Sopron, Vas, Veszprém, Somogy, and Fejér counties), together with Bács-Kiskun county in the South-Central part of Hungary (0.68% prevalence; 95% CI: 0–2.0%) (Figure 8). Positive samples were identified in eight out of 73 blood donating locations. The most affected cities were Szolnok (Jász-Nagykun-Szolnok county), Sopron (Győr-Moson-Sopron county), and Répcelak (Vas county), with three (two confirmed and one probable cases) and two seropositive donors, respectively. In the countryside, we found one seropositive donor each in Veszprém, Siófok, Kecskemét, and Székesfehérvár, and there was also one donor with a reactive result in the

capital, Budapest. The registered residency of positive donors was in close proximity to the place of blood donation (average distance, 21.28 km).

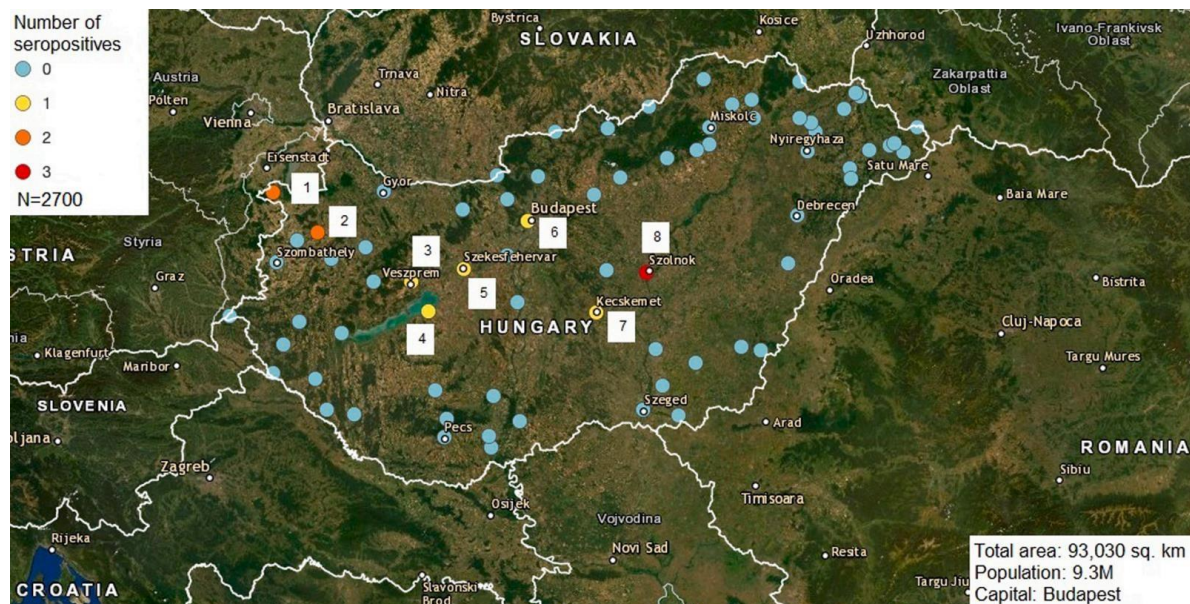


Figure 8. CCHF seroprevalence in Hungary and location of blood donation. Affected NUTS3 regions: 1–Győr-Moson-Sopron, 2–Vas, 3–Veszprém, 4–Somogy, 5–Fejér, 6–Budapest, 7–Bács-Kiskun, and 8–Jász-Nagykun-Szolnok. Light blue circle: no positive sample, Yellow: 1 positive sample, Orange: 2 positive samples, Red: 3 positive samples [71]. Visualization: EMMa Tool [69].

### 4.3. Animal serosurveillance

#### 4.3.1. Sample pooling and screening

In total, 1905 serum samples were tested for anti-CCHFV IgG antibodies. From the cattle serum specimens ( $n = 1391$ ), 287 pools were made, including 2–5 samples per pool based on geolocation. From the sheep serum specimens, 105 pools with 2–5 samples per pool were created. During the first screening, six pools of cattle samples and one pool of sheep samples were reactive ( $n = 3$ ) or equivocal ( $n = 4$ ). Serum specimens of the reactive or equivocal pools were tested further individually. Among the cattle, a total of eight samples (from five pools) showed anti-CCHFV IgG reactivity in all three assays (the Abbexa ELISA Kit, the in-house IIFA, and the EUROIMMUN Mosaic IIFA) with titers of 1:20 and 1:40 (Table 3).

Among the sheep, three reactive samples (with both IIFA assays) originated from a single sample pool with final anti-CCHFV IgG titers of 1:160 and 1:320 (Table 4). In the seventh pool, which gave equivocal result in the first screening, no individual sample was confirmed to be reactive (Appendix Table 4 and Appendix Figures 3 and 4).

Table 3. Results of the serological screening for anti-CCHFV IgG antibodies among cattle, including the number of tested samples and the number of reactive samples for each NUTS3 region and district of origin, and the final anti-CCHFV IgG titer obtained with the IIFA tests. Samples that gave reactive results in all three assays (Abbexa ELISA Kit, in-house IIFA, and EUROIMMUN Mosaic IIFA) were classified as seropositive [72].

<b>NUTS3 region</b>	<b>District of origin</b>	<b>Number of tested animals</b>	<b>Number of positive animals</b>	<b>IIFA titers</b>
Bács-Kiskun	Kecskemét	14	0	n.a.
	Baja	14	3	1:40
	Kiskunfélegyháza	14	0	1:40
	Kiskunhalas	28	0	n.a.
	Kalocsa	2	0	n.a.
Békés	Gyula	65	0	n.a.
	Mezőkovácsháza	18	0	n.a.
	Sarkad	1	0	n.a.
	unknown	50	0	n.a.
Borsod-Abaúj-Zemplén	Szerencs	5	0	n.a.
Csongrád	Hódmezővásárhely	28	0	n.a.
	Csongrád	18	1	1:40
Győr-Moson-Sopron	Csorna	14	3	1:20 - 1:40
	Mosonmagyaróvár	1	0	n.a.
Hajdú-Bihar	unknown	11	0	n.a.
	Törökszentmiklós	54	0	n.a.

Jász- Nagykun- Szolnok	Jászberény	13	0	n.a.
	Szolnok	79	0	n.a.
	Karcag	3	0	n.a.
	unknown	457	0	n.a.
Fejér	Mór	1	0	n.a.
	Sárbogárd	2	0	n.a.
	unknown	30	0	n.a.
Komárom- Esztergom	Komárom	30	0	n.a.
	Esztergom	12	0	n.a.
Nógrád	Salgótarján	15	0	n.a.
Veszprém	Pápa	6	0	n.a.
	Ajka	28	0	n.a.
	Veszprém	17	0	n.a.
	Várpalota	26	1	1:40
Pest	Aszód	14	0	n.a.
	Monor	57	0	n.a.
	Dabas	215	0	n.a.
	Cegléd	16	0	n.a.
Zala	unknown	33	0	n.a.
SUM		1391	8	

\*n.a.: not applicable.

Table 4. Results of the serological screening for anti-CCHFV IgG antibodies among sheep, including the number of tested samples and the number of reactive samples for each NUTS3 region and district of origin, and the final anti-CCHFV IgG titer obtained with the IIFA tests. Samples that gave reactive results in both assays (in-house IIFA and EUROIMMUN Mosaic IIFA) were classified as seropositive [72].

<b>NUTS3 region</b>	<b>District of origin</b>	<b>Number of tested animals</b>	<b>Number of positive animals</b>	<b>IIFA titers</b>
Bács-Kiskun	Tisza­kécske	44	0	n.a.
	Kiskunfélegyháza	60	3	1:160 – 1:320
	Kecskemét	96	0	n.a.
	Kiskunhalas	62	0	n.a.
Békés	Gyula	62	0	n.a.
Hajdú-Bihar	Nyíradony	95	0	n.a.
	Püspökladány	35	0	n.a.
Fejér	Dunaújváros	60	0	n.a.
SUM		514	3	

\*n.a.: not applicable.

#### 4.3.2. Geographical distribution

Samples were received from 13 NUTS3 regions, including 34 districts, mainly from the eastern and central parts of Hungary, with only a limited number of samples being available from the western and northern regions (Figure 9). For 514 cattle samples, the origin was known only at the NUTS3 region level. Among these cattle, seropositive samples were identified in five districts from four NUTS3 regions: one animal from the Csongrád district (Csongrád county), three animals from the Baja and Kiskunfélegyháza districts (Bács–Kiskun county), three animals from Csorna district (Győr–Moson–Sopron county), and one from Várpalota district (Veszprém county) showed seropositivity.

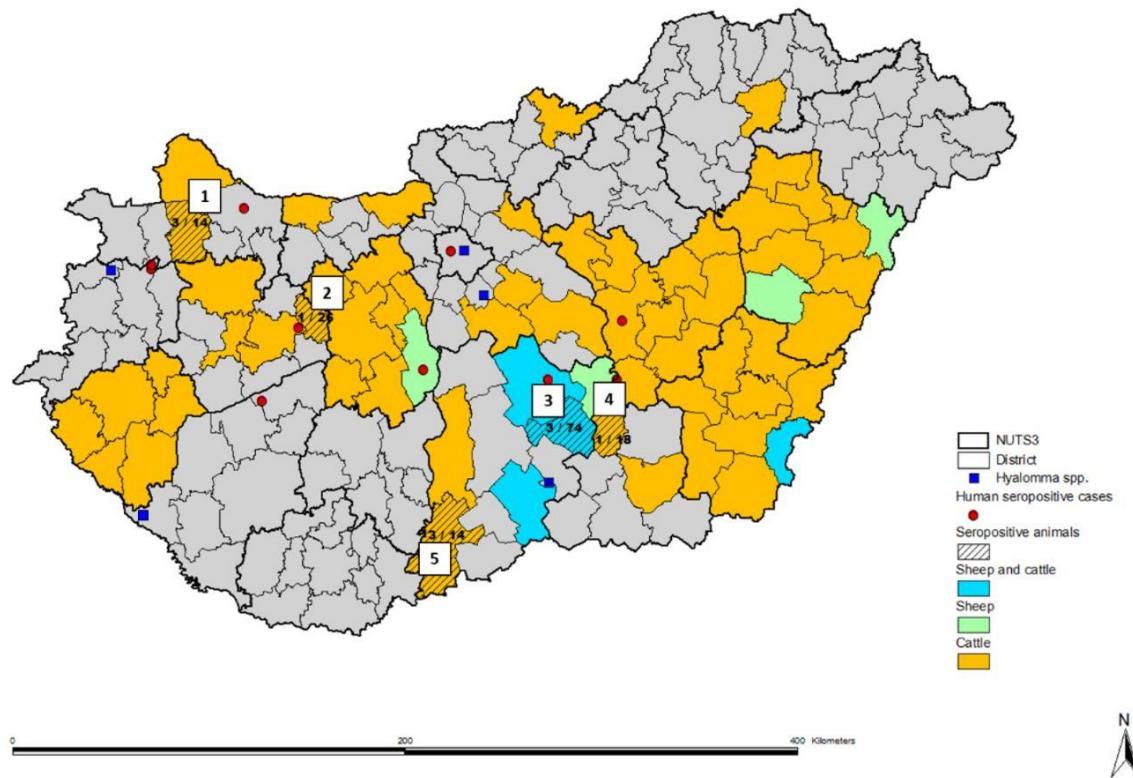


Figure 9. Map of Hungary showing administrative districts. Cattle and sheep serum samples were received from districts highlighted in orange and green, respectively. From four districts, both cattle and sheep samples were available for testing (highlighted in blue). The whole NUTS3 region is highlighted if the origin of the samples was known only at the NUTS3 level. Streaked districts represent regions with seropositive animals (1–Csorna, Győr–Moson–Sopron county; 2–Várpalota, Veszprém county; 3–Kiskunfélegyháza, Bács–Kiskun county; 4–Csongrád, Csongrád county; 5–Baja, Bács–Kiskun county) [72]. Red dots represent data of identified CCHFV seropositive human blood donors. Blue squares show historical data on the identification of *Hyalomma spp.* ticks in Hungary [47, 49-51].

Sheep serum samples were received from four NUTS3 regions, including eight districts. We found three seropositive samples from the Kiskunfélegyháza district (Bács–Kiskun county) (Figure 9).

The highest number of seropositive animals, including both cattle and sheep were found in Bács–Kiskun country in the south–central part of Hungary, with an average seropositivity of

1.8% (95% CI: 1.60–1.99%) among the tested animal population. The overall seropositivity of the tested animals in the affected NUTS3 regions (Csongrád, Bács-Kiskun, Győr-Moson-Sopron and Veszprém) was 2.33% (95% CI: 2.12–2.54%).

## 5. Discussion

Crimean-Congo hemorrhagic fever virus is a great public health concern in many countries worldwide, as it is one of the most widespread tick-borne viral pathogens with potentially severe symptoms and high consequence infection. In Hungary, only limited historical data was available regarding CCHFV circulation, and no human infection has been confirmed so far. As multiple species of the principal tick vectors have been identified in the country, it was highlighted as an area in need of CCHFV surveillance among the human and animal populations in 2015 [22, 47, 49-51]. To strengthen the capacity of CCHFV diagnosis in Hungary, the National Biosafety Laboratory developed and validated diagnostic methods, including an unbiased NGS protocol and an indirect immunofluorescent assay produced in-house.

### 5.1. In vitro growth-induced adaptation to cell lines

By introducing CCHFV WGS in our laboratory, we aimed to investigate the links between infectivity and phenotypic properties of the CCHFV and long-term genetic virus conservation or host-adaptation. As genome-based virus research forms the basis of robust and reliable approaches of novel diagnostics, antiviral and vaccine development, the highly variable genetic properties of the CCHFV makes it particularly important to identify potential genotypic and phenotypic changes during *in vitro* routine propagation of the virus [11, 64]. We designed a mutation accumulation study with serial virus propagation over ten generations and subsequent whole genome sequencing to map genetic diversity and promote the selection and emergence of different virus variants within a viral cloud. Cell susceptibility to CCHFV has been previously demonstrated in the case of a wide range of cell lines, however the changes in the genetic composition of the virus caused by *in vitro* serial passaging and adaption has not been studied before [73-78]. We compared three different MOI values during the first infection (MOI 0.005, 0.01, 0.1) in four different cell lines that are commonly used for CCHFV propagation (Vero E6, Vero, SW13 and BHK-21 cells). Our results showed that, the maximum virus copy number per mL was independent of the initial MOI as it increased to the same level due to the limiting effect of the susceptible cell

count. Furthermore, the inhibiting effect of the defective interfering particles (DIPs), as products of spontaneous error-prone virus replication of RNA viruses, such as CCHFV was also described in the literature. DIPs play important role during *in vitro* and *in vivo* infection, interfering with active virus replication and prompting persistence, especially during infection initiated at high MOI. Therefore, emergence of DIPs during replication can influence the logarithmic increase in virus titers [80]. We also compared the maximum infective titers for each cell line and it was the highest in SW13 cells. Furthermore, we detected CPE only in SW13 cells, which was consistent with the findings of Dai *et al.* and Agol *et al.* [73, 79]. The infection in SW13 cells may induce a host-encoded necrotic program as an anti-CCHFV response, while the CPE may be attributed to host-defense and anti-viral defense, not directly caused by viral reproduction [73]. Virus infective titer rapidly decreased after CPE, which may because the virus stability shows rapid reduction in wet conditions (cell-free culture medium) at 37°C, and loses infectivity completely after 7 hours [81].

Considering that the highest logarithmic increase in the infective titers and viral RNA copies were found when infected at MOI 0.005, we performed the subsequent serial passages (P2-P10) at MOI 0.005, as producing higher virus yield favors diversity and mutation accumulation [11]. Our data strongly corresponded with the findings of Dai *et al.*, who showed that SW13, Vero and Vero E6 cells are highly permissive, and BHK-21 is a permissive cell line for CCHFV [73]. In our experiment, the highest increase in permissivity was seen in Vero cells with a 1.99 log growth attributed to long-term adaptation.

In order to map the genetic variations potentially underlying these phenotypic changes, whole genome sequencing was performed by using the unbiased SISPA enrichment methodology followed by paired-end Illumina sequencing. While it has been suggested that the SISPA technique has the potential to introduce sequencing errors [66, 82, 83], it was shown that the methodology can affect the sequencing depth in genome regions of high complexity and GC-content rather than the amplification bias [66, 82-85].

During the whole genome analysis, we calculated the average VF and plotted the variant distribution against genome segments in all the samples. Whereas higher VF based on low number of mutations suggests host-adaptation and gain of fitness, lower VF over high number of mutations could indicate the persistence of quasi-species serving the basis for the

selection of virulent variants [86]. The highest increase in the average VF over serial propagation was seen when passaged in BHK-21 cells (4.9%), which can also explain the significant increase in the permissivity of the cell line to CCHFV (1.3 log) through host-adaptation. In contrast, average VF decreased in SW13 cells (0.42%) along with permissivity to CCHFV (0.81 log) during serial propagation.

Growth-adaptive mutations were described for other RNA viruses, as well. Gain-of-entry function mutations were identified in the Ebola virus Makona strain glycoprotein region when passaged in Huh-7 and Vero E6 cell lines. Furthermore, a tissue culture-specific spontaneous mutation (T544I) recognized in the Ebola virus GP showed no effect in the pathogenesis, but remained fixed in the viral genome after three passages *in vivo* [87, 88]. In the case of West Nile virus, the replicative fitness increased significantly and resulted in non-synonymous mutations in a temperature-dependent manner, when the virus was *in vitro* passaged 12 times in *Culex tarsalis* cells at 25°C and 30°C [89]. Furthermore, as Nemirov *et al.* demonstrated for Puumala Hantavirus, which also belongs to the *Nairoviridae* family, that mutations in the L segment and the non-coding region of the S segment emerged during serial passaging in Vero E6 cells. They found that the population of L RNA molecules is represented by quasispecies. It was also shown that one mutation in the L segment contributes to a better replication of Hantaan virus in suckling mice and thus increases its virulence, which phenomenon indicated fluctuating levels of quasispecies that evolve and adapt to the host cell [90]. In the present study, we also found the highest average VFs in the CCHFV L segment with high deviation among cell lines.

In the S segments, we found only one unique synonym SNP (I448I) with a frequency over 40% attributed to virus adaptation to BHK-21 cell line, however the overall average frequency was low (16.35%) in this segment. Our data indicates that adaptation to specific cell lines attributed to the variations in the viral nucleoprotein emerge at the low-frequency quasi-species level, and not at consensus level. In the M segment, we found three nt variations with frequencies over 40% (L276L, E594K and D1168G) that emerged only after the first cross-passages. All consensus level mutations emerged when the virus was propagated in Vero cells (L276L, E594K, D1168G) might also supporting enhanced permissivity. Non-synonym mutations E594K and D1168G emerged in the Gn and Gc

regions, respectively, and might have potential effect on cell entry or virus neutralization efficacy. Furthermore, mutation D1168G falls on the glycoprotein nucleolin binding site [7]. However, biological relevance of these mutations needs further investigation. We found the lowest average VF in the M segment (15.53%) compared to the other genome segments, but the number of nt variations per kb genome was the highest (1.77 SNP/kb); suggesting that adaptation to new host cell lines may be attributed to the slow emergence of viral quasi-species in the Gn and Gc proteins responsible for receptor binding. In the L segment, the overall average frequency was the highest (33.74%) among segments, with low mutation number per kb (1.13 SNP/kb). The highest increase in the VF was observed when cross-passaged from BHK-21 cells, suggesting the emergence of new, high-frequency nt variants. Non-synonym mutation A2279V (that emerged when serial passaging in BHK-21 cells) close to the RdRp catalytic region is particularly interesting, and needs further studying to unfold biological relevance.

The results of the genomic variations comply with the phenotypic changes observed in the virus permissivity, which also showed an increase for BHK-21 and Vero cells due to serial passaging. It is also important to note, that CPE caused by virus propagation was only observed in SW13, in which cells with the highest initial permissivity was seen.

To further investigate host-adaptation, we analyzed the abundance of nucleotide change preferences of CCHFV. Codon usage bias as the product of mutation pressure and/or natural selection for accurate and efficient translation, protein secondary motifs, replication, etc. was previously demonstrated to be weak in the case of CCHFV. Some similarities were found between the codon usage patterns of the virus and its natural hosts such as humans and ticks, but the viral adaptation mechanisms was not investigated further [91-93]. We identified T>C as the most common nucleotide change, which accounts for 22.44% of all SNPs, while A>G accounts for 21.44%. Both mutation types are transitions. A>C transversions were also common (13.44% overall prevalence), especially in the M segment (24.76%). Growth-adaptive high frequency nt change was affected by the new host cell line, which correlates with the results of Rahman *et al.*, who found the nucleotide composition of the virus to be host-dependent, based on the analysis of 179 CCHFV whole genomes derived from infected human (*Homo sapiens*), *Hyalomma* tick, cattle (*Bos taurus*) and sheep (*Ovis aries*) samples

[91]. It is important to note that the new cell line also affected the virus growth kinetics after cross-passaging, which may be related to the nt change preference in certain cell lines.

Silent mutations in the third nucleotide position are often retrieved from adaptation mechanisms to the host organism to evade immunological response [94]. We found that the majority of the silent mutations (3 out of 4) above 40% frequency are linked to BHK-21 or Vero adaptation. One silent mutation (I448I) in the S segment emerged when passaged in BHK-21, but reverted in all other cell lines. In the M segment, one silent consensus level SNP (L276L) was identified and attributed to Vero-adaptation. Two additional non-silent mutations (E594K, D1168G) emerged Vero E6-specifically in the Gn and Gc regions. In the L segment, silent ( $n = 4$ ) and non-silent ( $n = 6$ ) mutations have evolved in a cell line specific manner. Among silent nt mutations, two emerged when passaged in BHK-21 cells (P889P, F2576F).

## 5.2. Human and animal serosurveillance

With the use of our IIFA test, we set up a pilot retrospective serosurvey among defined human and animal populations (healthy volunteer blood donors and free-range indicator animals, including cattle and sheep) to obtain information about the seroprevalence of CCHFV infection in Hungary. A systematic review published in 2019 summarized worldwide CCHFV seroprevalence data obtained between 1969 and 2018. Seroprevalence in the general human population was estimated between 0.1-14.4% with higher seropositivity rates in hyperendemic countries, such as Turkey, Iran, and Afghanistan. The mean seroprevalence in the examined areas was 4.4% (SD  $\pm$ 2.4) calculated based on published data, and showed an overall increasing tendency in the last decade [43, 107]. For example, in Bulgaria, seropositivity increased between 2011 and 2015 from 2.8% to 3.7% among the general human population with simultaneous increase in the geographic spread [43-46].

According to the WHO, there is no standardized serological method for human CCHF diagnosis; however, IIFA based on the whole virus is the most commonly used method [3, 60]. Two independent studies published in 2012 and 2014 state that most of the European reference laboratories with the capacity to diagnose CCHFV infection use in-house IIFA kits for serology [95, 96]. Fifty percent of the laboratories that use commercially available ELISA

kits also claim to combine the results of commercial kits with those of in-house serology assays, which may compensate for potential reductions in sensitivity caused by the antigenic diversity of CCHFV [95]. Retrospective serological testing is also complicated by the unique phenomenon that in the case of certain individuals, antibodies are produced either only against the NP antigen, while in others only against the GPC. Many in-house and commercial ELISA kits have been published containing mostly the NP or GPC viral antigens. In the case of indirect immunofluorescent assays (IIFA), in-house IIFA slides contain the whole virus with all its antigens, while commercial assays contain transfected cells with NP and/or GPC viral antigens [97].

During our work, we tested 2700 serum samples taken from healthy volunteer blood donors between 2008 and 2017 and screened them for anti-CCHFV IgG antibodies using an IIFA and a commercial recombinant ELISA kit. Our results show that male donors were more affected, with a seroprevalence of 0.55% compared with 0.16% among female donors. This may be due to the fact that men are more likely to work in professions with an occupational risk of exposure to infected ticks or animals. As Chinikar *et al.* suggested, high-risk behaviors and professions often associated with men, such as foresting, hunting, slaughtering, or animal handling can facilitate transmission of the disease [100]. However, we obtained no information about the profession of the donors. In hyperendemic areas of Kosovo that have high seroprevalence, 70% of seropositive individuals are men who have probably been exposed to CCHFV infection during professional activities such as farming or slaughtering [98]. As Nasirian *et al.* determined the total mean of CCHFV seroprevalence for at-risk professionals in endemic areas (including Iran, Turkey, Georgia and Greece) was 30.3% among animal workers, 16.5% among butchers and slaughterhouse workers, and 36.5% among farm workers. The total mean of CCHFV seroprevalence of confirmed patients or patient-related contact populations in Turkey was 85.0%. Furthermore, animal contact was also often associated with increased CCHFV seropositivity [107].

Regarding age, the seroprevalence was higher in the youngest group in our study. Considering geographical distribution, positive samples were found in 40% of NUTS3 regions in Hungary, with a prevalence of between 0.20% and 2.97%, with the western and central parts of the country being the most affected. The highest seroprevalence was observed

in Jász-Nagykun-Szolnok region (2.97%), which is situated in the Great Plain of central Hungary. However, we cannot rule out the possibility that the place of donation and/or residence, and/or the place of exposure to CCHFV were different; this is because many donors donate blood near their residency, but may have been exposed while visiting rural areas. The registered residency of positive donors was in close proximity to the place of blood donation (average distance, 21.28 km).

Serological surveys among animals also bear important predictive value, as they serve as the principal source of information to monitor areas with natural virus transmission and to identify exposed species. Among vertebrates, the highest seropositivity was found among sheep and goats (24.3% and 29.3%, respectively), while it was lower among cattle (18.9%) based on historical data reported from multiple endemic or potentially endemic counties [43, 107].

Several publications found evidence of CCHFV circulation in Hungary among animals; a local study focusing on the southeastern region of the country found serological evidence of CCHFV among European brown hares (*Lepus europaeus*) collected between 2008 and 2009 [53]. Another survey testing wild rodents captured between 2011 and 2013 in the Mecsek Mountain region found 0.96% seroprevalence using dot-blot and immunofluorescence assays [54]. The number of seropositive animals is also high in some neighboring areas of Hungary. In southern Romania, a study performed between 2019 and 2020 assessed the seroprevalence of CCHFV in 250 sheep and goats using ELISA; the results showed an overall 37.7% antibody positivity [101]. In Albania, a study published in 2014, reported 46% seropositivity in sheep and 28% in goats [24]. In North Macedonia, the seropositivity among cattle was estimated to be as high as 80% in the northeastern part of the country, including 75% in sheep and 59% in goats [102]. In Bulgaria, high CCHFV seroprevalence was also detected in cattle, goats, and sheep, with 19.6%, 22.7%, and 7.7% IgG positivity, respectively [103].

Gaining data on the levels of seropositivity among animals is particularly important from the One Health aspect, as several cases of primary human infections are described where the person came into direct contact with the infectious body secretions of the infected animal or removed an infected tick and consequently became infected with CCHFV [26, 100, 104, 105]. Furthermore, secondary nosocomial infections have also been described where the

index case occurred due to direct contact with an infected animal or tick bite. Then, the medical staff involved in the treatment also acquired CCHFV infection [38, 106]. According to a systematic review published in 2019, the global trend of CCHFV seroprevalence in livestock showed an increase over time (between 1969 and 2018), with 10.0–27.0%, 19.0–41.0%, and 0.5–37.0% for camels, sheep, and livestock, respectively. In cattle and goats it exhibited a slightly increasing trend, with 16.5–21.0 and 22.0–27.0%, respectively [107]. Tendency of CCHFV infections attributed to secretion exposure also increased between 2009 and 2017 in the CCHFV endemic areas (Turkey, Afghanistan, Georgia, Iran) and ranged between 18.5 and 57.9% of all detected cases [107]. Furthermore, investigations into human infections in endemic areas often revealed elevated CCHFV seroprevalence in local livestock [42, 107].

During our serosurvey among free-range vertebrates, sera from the same geolocations were tested in pools containing two to five samples per pool, which may lead to reduced sensitivity. To overcome this, we used multiple serological assays with low initial sample dilutions (1:5 for the ELISA kit and 1:20 for the IIFA kits) to increase sensitivity. Among 1391 tested cattle and 514 sheep serum samples, we found 0.57% and 0.58% to be seropositive, respectively. We found CCHFV seropositive animals in the south–central (Bács-Kiskun) and (north)-western (Győr-Moson-Sopron and Veszprém) regions of Hungary. The overall seropositivity was 2.33% in the affected NUTS3 regions. Interestingly, all identified seropositive sheep samples ( $n = 3$ ) were received from the same location (Kiskunfélegyháza), where we also detected a seropositive cow and found anti–CCHFV IgG positive human blood donors as well. Regarding geographical distribution, our data obtained in the frame of the animal serosurveillance correlate with our results on the CCHFV seroprevalence among the general human population, and are also comparable with the historical reports of the primary vector, the *Hyalomma* ticks in Hungary. Although the seroprevalence determined both in the human population and among indicator animals can be considered low, especially compared to the seroprevalence data in certain hyper-endemic areas, it clearly indicates some degree of CCHFV presence in the country. As more than 80% of CCHFV infections are asymptomatic or with mild symptoms and remain undiagnosed, potential virus circulation can only be monitored through retrospective serosurveillance.

## 6. Conclusions

Based on previously reported data, Hungary stands within high evidence consensus in the aspect of CCHFV transmission and circulation. Thus, we aimed to incorporate international recommendations and requirements into our CCHFV research. To do so, we studied phenotypic and genotypic changes in the CCHFV genome in a stable and controlled cellular environment. The methods of serial passaging and next generation sequencing allowed us to identify mutations at low frequency arising across the entire viral genome, as expected for RNA viruses with a high error rate during replication. By focusing on the mutations that reached consensus level frequency concomitant with the adapted phenotype, we were able to combine CCHFV propagation in controlled laboratory settings with phenotypic characterization, in order to better understand *in vitro* viral evolution and possible adaptation to commonly used cell lines, that might influence the approaches of novel diagnostic, antiviral and vaccine development in laboratory settings. As changes in the viral genome and the emergence of new viral quasi-species can affect virus properties, such as pathogenicity, fitness, host-adaptation, evasion of the immune response, enhanced host-cell permissivity, etc., genetic variations have impact on the sensitivity and specificity of certain diagnostic tests. Any mutation in the primer-binding region can reduce primer-binding affinity, leading to decreased specificity and sensitivity of the NAATs and result in false negativity, especially in the case of clinical samples with low initial viral load. Therefore, it is particularly important to recognize the appropriate non-variable genome regions as potential diagnostic targets in the case of highly diverse RNA viruses, such as CCHFV. Genetic variations can interfere with viral antigen and antibody detection assays as well. The altered genetic properties can lead to altered antigenic properties that may result in weakened antigen-antibody binding reaction that serves as basis for serological assays. Hence, tests containing all viral antigens and polyclonal antibodies against multiple epitopes can be considered better and more feasible diagnostic options.

As part of our research, we performed the first retrospective and systematic CCHFV serosurveys focusing on human and animal populations in Hungary covering a significant geographical area, in order to address the gap in the serosurveillance programs, highlighted

by several publications [55-57]. Although the serum samples were taken before 2017, we obtained essential data on the CCHFV serological status in Hungary from a few years ago. In relation to the increasing seropositivity in the south and south-east of Hungary, and based on other risk factors, such as vector presence, climatic features, and serological evidence, the probability of the potential introduction and subsequent human CCHFV infection in the country is significant [22, 47-54]. The results of our pilot serosurveys can serve as a basis for a systematic, cross-sectorial serosurveillance program focusing on at-risk human, animal, and tick populations. Furthermore, based on our newly generated data, Hungary is now categorized as a level 3 (high potential) country considering the risk of CCHFV introduction and future human infections. As next step, we would like to assess the current seroprevalence in the country to gain important information regarding the spatio-temporal emergence of CCHFV since 2017. We also aim to perform active and comprehensive surveillance focusing on the principal tick vectors present and the CCHFV strains that potentially circulate in the affected geographical areas of Hungary. Moreover, our results highlight the importance of raising awareness among healthcare workers and other at-risk populations of the emerging threat of CCHFV in Hungary and Central Europe.

## 7. Summary

As CCHFV shows enhanced genetic diversity that can result in the emergence of viral quasi-species, one of our aims was to determine the replication kinetics and genetic variations resulted by *in vitro* serial passaging in susceptible cell lines. This task is an important quality management issue, as genetic variations may lead to phenotypic changes regarding infectivity and viral fitness. In the frame of this thesis:

- We established a mutation accumulation experiment in four susceptible cell lines (Vero E6, Vero, SW13, BHK-21), followed by deep sequencing and analysis to map signature mutations.
- We found that all tested cell lines are susceptible for CCHFV, and permissivity increased due to serial passaging in Vero and BHK-21 cells.
- Growth-induced mutations emerged in a cell-line specific manner, as the applied cell lines had significant effect on the mutation variant frequency. By mapping growth-induced mutations, we were able to combine viral evolution in controlled laboratory settings with phenotypic characterization.

As Hungary stands within high evidence consensus for future CCHFV introduction and human infection, we aimed to assess CCHFV seropositivity among humans and indicator animals in the country. In the frame of this thesis:

- In total, 2700 human and 1905 serum samples taken from free-range cattle and sheep were tested for anti-CCHFV IgG antibodies using a range of commercial in-house assays. We found a total of 10 reactive samples among humans (0.44%) and 11 reactive samples (0.58%) among animals comprising 8 cattle and 3 sheep. The most affected regions were the south-central and northwestern parts of the country.
- Based on our newly generated data, Hungary is now categorized as a level 3 (high potential) country considering the risk of CCHFV introduction and future human infections.

Accordingly, a more extended surveillance is advised, especially in the affected areas, and there should be greater awareness among clinicians and other high-risk populations of the emerging threat of CCHFV in Hungary and Central Europe.

## 8. References

- [1] International Committee for Virus Taxonomy (ICTV): Family: Nairoviridae Genus: Orthonairovirus. Available online: <https://ictv.global/report/chapter/nairoviridae/nairoviridae/orthonairovirus> (last access: 31 January 2025).
- [2] Magyar N. (2022): Chapter 27. *Nairoviridae*. In Takács M (Ed).: Orvosi Virologia (Medicina Kiadó). 2022;pp255-258.
- [3] World Health Organization: Crimean-Congo haemorrhagic fever. Available online: <https://www.who.int/news-room/fact-sheets/detail/crimean-congo-haemorrhagic-fever> (last access 16 December 2024).
- [4] World Health Organization: Crimean-Congo Haemorrhagic Fever (CCHF) Research and Development (R&D) Roadmap. Available online: [https://cdn.who.int/media/docs/default-source/blue-print/cchf\\_rdblueprint\\_roadmap\\_advanceddraftnov2019.pdf?sfvrsn=aa5356a\\_3&download=true](https://cdn.who.int/media/docs/default-source/blue-print/cchf_rdblueprint_roadmap_advanceddraftnov2019.pdf?sfvrsn=aa5356a_3&download=true) (last access: 16 December 2024).
- [5] Fields BN. (ed), 2013. Field's Virology. 6th Edition. Lippincott Williams and Wilkins, Philadelphia, USA.
- [6] Zivcec M, Scholte FE, Spiropoulou CF, Spengler JR, Bergeron É. Molecular Insights into Crimean-Congo Hemorrhagic Fever Virus. *Viruses*. 2016 Apr 21;8(4):106. doi: 10.3390/v8040106.
- [7] Hawman DW, Feldmann H. Crimean-Congo haemorrhagic fever virus. *Nat Rev Microbiol*. 2023 Jul;21(7):463-477. doi: 10.1038/s41579-023-00871-9.
- [8] Welch SR, Scholte FEM, Spengler JR, Ritter JM, Coleman-McCray JD, Harmon JR, Nichol ST, Zaki SR, Spiropoulou CF, Bergeron E. The Crimean-Congo Hemorrhagic Fever Virus NSm Protein is Dispensable for Growth In Vitro and Disease in Ifnar<sup>-/-</sup> Mice. *Microorganisms*. 2020 May 21;8(5):775. doi: 10.3390/microorganisms8050775.

- [9] Kong Y, Yan C, Liu D, Jiang L, Zhang G, He B, Li Y. Phylogenetic analysis of Crimean-Congo hemorrhagic fever virus in inner Mongolia, China. *Ticks Tick Borne Dis.* 2022 Jan;13(1):101856. doi: 10.1016/j.ttbdis.2021.101856.
- [10] Carroll SA, Bird BH, Rollin PE, Nichol ST. Ancient common ancestry of Crimean-Congo hemorrhagic fever virus. *Mol Phylogenet Evol.* 2010 Jun;55(3):1103-10. doi: 10.1016/j.ympev.2010.01.006.
- [11] Stern A, Andino R. Viral Evolution: It Is All About Mutations (Chapter 17) in *Viral Pathogenesis (Third Edition)*. Katze MG, Korth MJ, Law GL, Nathanson N (eds). 2016 Elsevier.
- [12] Rahman SU, Yao X, Li X, Chen D, Tao S. Analysis of codon usage bias of Crimean-Congo hemorrhagic fever virus and its adaptation to hosts. *Infect Genet Evol.* 2018 Mar;58:1-16. doi: 10.1016/j.meegid.2017.11.027.
- [13] Government of Canada: Crimean-Congo hemorrhagic fever virus: Infectious substances pathogen safety data sheet. Available online: <https://www.canada.ca/en/public-health/services/laboratory-biosafety-biosecurity/pathogen-safety-data-sheets-risk-assessment/crimean-congo-haemorrhagic-fever-virus.html> (last access 16 December 2024).
- [14] Xu ZS, Du WT, Wang SY, Wang MY, Yang YN, Li YH, Li ZQ, Zhao LX, Yang Y, Luo WW, Wang YY. LDLR is an entry receptor for Crimean-Congo hemorrhagic fever virus. *Cell Res.* 2024 Feb;34(2):140-150. doi: 10.1038/s41422-023-00917-w.
- [15] Monteil VM, Wright SC, Dyczynski M, Kellner MJ, Appelberg S, Platzer SW, Ibrahim A, Kwon H, Pittarokoilis I, Mirandola M, Michlits G, Devignot S, Elder E, Abdurahman S, Bereczky S, Bagci B, Youhanna S, Aastrup T, Lauschke VM, Salata C, Elaldi N, Weber F, Monserrat N, Hawman DW, Feldmann H, Horn M, Penninger JM, Mirazimi A. Crimean-Congo haemorrhagic fever virus uses LDLR to bind and enter host cells. *Nat Microbiol.* 2024 Jun;9(6):1499-1512. doi: 10.1038/s41564-024-01672-3.
- [16] Bente, D.A.; Forrester, N.L.; Watts, D.M.; McAuley, A.J.; Whitehouse, C.A.; Bray, M. Crimean-Congo hemorrhagic fever: History, epidemiology, pathogenesis, clinical syndrome

and genetic diversity. *Antiviral Res.* 2013, 100, 159–189. <https://doi.org/10.1016/j.antiviral.2013.07.006>.

[17] Negredo A, de la Calle-Prieto F, Palencia-Herrejón E, Mora-Rillo M, Astray-Mochales J, Sánchez-Seco MP, Bermejo Lopez E, Menárguez J, Fernández-Cruz A, Sánchez-Artola B, Keough-Delgado E, Ramírez de Arellano E, Lasala F, Milla J, Fraile JL, Ordobás Gavín M, Martínez de la Gándara A, López Perez L, Diaz-Diaz D, López-García MA, Delgado-Jimenez P, Martín-Quirós A, Trigo E, Figueira JC, Manzanares J, Rodríguez-Baena E, García-Comas L, Rodríguez-Fraga O, García-Arenzana N, Fernández-Díaz MV, Cornejo VM, Emmerich P, Schmidt-Chanasit J, Arribas JR; Crimean Congo Hemorrhagic Fever@Madrid Working Group. Autochthonous Crimean-Congo Hemorrhagic Fever in Spain. *N Engl J Med.* 2017 Jul 13;377(2):154-161. doi: 10.1056/NEJMoa1615162.

[18] Logan, T.M.; Linthicum, K.J.; Bailey, C.L.; Watts, D.M.; Moulton, J.R. Experimental transmission of Crimean-Congo hemorrhagic fever virus by *Hyalomma truncatum* Koch. *Am. J. Trop. Med. Hyg.* 1989, 40, 207–212. <https://doi.org/10.4269/ajtmh.1989.40.207>.

[19] European Centre for Disease Prevention and Control: *Hyalomma marginatum* - current known distribution: August 2023. Available online: <https://www.ecdc.europa.eu/en/publications-data/hyalomma-marginatum-current-known-distribution-august-2023> (last access 16 December 2024).

[20] Hornok, S.; Flaisz, B.; Takács, N.; Kontschán, J.; Csörgő, T.; Csipak, Á.; Jaksa, B.R.; Kováts, D. Bird ticks in Hungary reflect western, southern, eastern flyway connections and two genetic lineages of *Ixodes frontalis* and *Haemaphysalis concinna*. *Parasit. Vectors* 2016, 9, 101. <https://doi.org/10.1186/s13071-016-1365-0>.

[21] Ergönül, O. Crimean-Congo haemorrhagic fever. *Lancet Infect. Dis.* 2006, 6, 203–214. [https://doi.org/10.1016/S1473-3099\(06\)70435-2](https://doi.org/10.1016/S1473-3099(06)70435-2).

[22] Messina JP, Pigott DM, Golding N, Duda KA, Brownstein JS, Weiss DJ, Gibson H, Robinson TP, Gilbert M, William Wint GR, Nuttall PA, Gething PW, Myers MF, George DB, Hay SI. The global distribution of Crimean-Congo hemorrhagic fever. *Trans R Soc Trop Med Hyg.* 2015 Aug;109(8):503-13. doi: 10.1093/trstmh/trv050.

- [23] Whitehouse, C.A. Crimean-Congo hemorrhagic fever. *Antiviral Res.* 2004, 64, 145–160. <https://doi.org/10.1016/j.antiviral.2004.08.001>.
- [24] Lugaj, A.; Koni, M.; Mertens, M.; Groschup, M.H.; Berxholi, K. Serological survey of Crimean-Congo hemorrhagic fever virus in cattle in Berat and Kolonje, Albania. *Albanian J. Agric. Sci.* 2014, 13, 325–328.
- [25] Fanelli, A.; Tizzani, P.; Buonavoglia, D. Crimean-Congo Haemorrhagic Fever (CCHF) in animals: Global characterization and evolution from 2006 to 2019. *Transbound. Emerg. Dis.* 2022, 69, 1556–1567. <https://doi.org/10.1111/tbed.14120>.
- [26] Habibzadeh, S.; Mohammadshahi, J.; Bakhshzadeh, A.; Moradi-Asl, E. The First Outbreak of Crimean-Congo Hemorrhagic Fever Disease in Northwest of Iran. *Acta Parasitol.* 2021, 66, 1086–1088. <https://doi.org/10.1007/s11686-021-00342-2>.
- [27] Portillo A, Palomar AM, Santibáñez P, Oteo JA. Epidemiological Aspects of Crimean-Congo Hemorrhagic Fever in Western Europe: What about the Future? *Microorganisms.* 2021 Mar 21;9(3):649. doi: 10.3390/microorganisms9030649.
- [28] Centers for Disease Control and Prevention (CDC): Crimean-Congo Hemorrhagic Fever (CCHF). Available online: <https://www.cdc.gov/vhf/crimean-congo/symptoms/index.html> (last access 16 December 2024).
- [29] Al-Abri SS, Abaidani IA, Fazlalipour M, Mostafavi E, Leblebicioglu H, Pshenichnaya N, Memish ZA, Hewson R, Petersen E, Mala P, Nhu Nguyen TM, Rahman Malik M, Formenty P, Jeffries R. Current status of Crimean-Congo haemorrhagic fever in the World Health Organization Eastern Mediterranean Region: issues, challenges, and future directions. *Int J Infect Dis.* 2017 May;58:82-89. doi: 10.1016/j.ijid.2017.02.018.
- [30] Hawman, D.W.; Feldmann, H. Crimean-Congo haemorrhagic fever virus. *Nat. Rev. Microbiol.* 2023, 21, 463–477. <https://doi.org/10.1038/s41579-023-00871-9>.
- [31] Bente, D.A.; Forrester, N.L.; Watts, D.M.; McAuley, A.J.; Whitehouse, C.A.; Bray, M. Crimean-Congo hemorrhagic fever: History, epidemiology, pathogenesis, clinical syndrome and genetic diversity. *Antiviral Res.* 2013, 100, 159–189. <https://doi.org/10.1016/j.antiviral.2013.07.006>.

- [32] Papa A, Marklewitz M, Paraskevopoulou S, Garrison AR, Alkhovsky SV, Avšič-Županc T, Bente DA, Bergeron É, Burt F, Di Paola N, Ergünay K, Hewson R, Mirazimi A, Sall AA, Spengler JR, Postler TS, Palacios G, Kuhn JH. History and classification of Aigai virus (formerly Crimean-Congo haemorrhagic fever virus genotype VI). *J Gen Virol.* 2022 Apr;103(4):001734. doi: 10.1099/jgv.0.001734.
- [33] Maltezou, H.C.; Papa, A. Crimean-Congo hemorrhagic fever: Risk for emergence of new endemic foci in Europe? *Travel Med. Infect. Dis.* 2010, 8, 139–143. <https://doi.org/10.1016/j.tmaid.2010.04.008>.
- [34] De Liberato, C.; Frontoso, R.; Magliano, A.; Montemaggiori, A.; Autorino, G.L.; Sala, M.; Bosworth, A.; Scicluna, M.T. Monitoring for the possible introduction of Crimean-Congo haemorrhagic fever virus in Italy based on tick sampling on migratory birds and serological survey of sheep flocks. *Prev. Vet. Med.* 2018, 149, 47–52. <https://doi.org/10.1016/j.prevetmed.2017.10.014>.
- [35] European Centre for Disease Prevention and Control: Cases of Crimean–Congo haemorrhagic fever infected in the EU/EEA, 2013–present. Available online: Cases of Crimean–Congo haemorrhagic fever infected in the EU/EEA, 2013–present (last access 16 December 2024).
- [36] International Society for Infectious Diseases (ProMED). E-mail alert: 2013-06-24. Crimean-Congo hemorrhagic fever - Kosovo Region: Travel alert.
- [37] Lorenzo Juanes HM, Carbonell C, Sendra BF, López-Bernus A, Bahamonde A, Orfao A, Lista CV, Ledesma MS, Negredo AI, Rodríguez-Alonso B, Bua BR, Sánchez-Seco MP, Muñoz Bellido JL, Muro A, Belhassen-García M. Crimean-Congo Hemorrhagic Fever, Spain, 2013-2021. *Emerg Infect Dis.* 2023 Feb;29(2):252-259. doi: 10.3201/eid2902.220677.
- [38] Eslava M, Carlos S, Reina G. Crimean-Congo Hemorrhagic Fever Virus: An Emerging Threat in Europe with a Focus on Epidemiology in Spain. *Pathogens.* 2024 Sep 6;13(9):770. doi: 10.3390/pathogens13090770.

- [39] Spengler, J.R., Bergeron ,É., Rollin, P.E., 2016a. Seroepidemiological studies of Crimean-Congo hemorrhagic fever virus in domestic and wild animals. *PLoS Negl. Trop. Dis.* 10, e0004210. <https://doi.org/10.1371/journal.pntd.0004210>
- [40] Schuster, I., Mertens, M., Mrenoshki, S., Staubach, C., Mertens, C., Brüning, F., Wernike, K., Hechinger, S., Berxholi, K., Mitrov, D., Groschup, M.H., 2016. Sheep and goats as indicator animals for the circulation of CCHFV in the environment. *Exp. Appl. Acarol.* 68, 337-346. doi: 10.1007/s10493-015-9996-y.
- [41] Spengler, J.R., Estrada-Peña, A., Garrison, A.R., Schmaljohn, C., Spiropoulou, C.F., Bergeron, É., Bente, D.A., 2016b. A chronological review of experimental infection studies of the role of wild animals and livestock in the maintenance and transmission of Crimean-Congo hemorrhagic fever virus. *Antiviral Res.* 135, 31-47. doi: 10.1016/j.antiviral.2016.09.013.
- [42] Nyakarahuka L, Kyondo J, Telford C, Whitesell A, Tumusiime A, Mulei S, Baluku J, Cossaboom CM, Cannon DL, Montgomery JM, Lutwama JJ, Nichol ST, Balinandi SK, Klena JD, Shoemaker TR. Seroepidemiological investigation of Crimean Congo hemorrhagic fever virus in livestock in Uganda, 2017. *PLoS One.* 2023 Nov 9;18(11):e0288587. doi: 10.1371/journal.pone.0288587. [43] Riccò M, Baldassarre A, Corrado S, Bottazzoli M, Marchesi F. Seroprevalence of Crimean Congo Hemorrhagic Fever Virus in Occupational Settings: Systematic Review and Meta-Analysis. *Trop Med Infect Dis.* 2023 Sep 19;8(9):452. doi: 10.3390/tropicalmed8090452.
- [44] Christova, I., Panayotova, E., Trifonova, I., Taseva, E., Hristova, T., Ivanova, V., 2017. Countrywide seroprevalence studies on Crimean-Congo hemorrhagic fever and hantavirus infections in general population of Bulgaria. *J. Med. Virol.* 89, 1720-1725. doi: 10.1002/jmv.24868.
- [45] Gergova, I., Kamarinchev, B., 2013. Comparison of the prevalence of Crimean-Congo hemorrhagic fever virus in endemic and non-endemic Bulgarian locations. *J. Vector Borne Dis.* 50, 265-270.

- [46] Gergova, I., Kamarinchev, B., 2014. Seroprevalence of Crimean-Congo hemorrhagic fever in southeastern Bulgaria. *Jpn. J. Infect. Dis.* 67, 397-398. doi: 10.7883/yoken.67.397.
- [47] Hornok, S.; Horváth, G. First report of adult *Hyalomma marginatum rufipes* (vector of Crimean-Congo haemorrhagic fever virus) on cattle under a continental climate in Hungary. *Parasit. Vectors* 2012, 5, 170. <https://doi.org/10.1186/1756-3305-5-170>.
- [48] Hornok, S.; Farkas, R. First autochthonous infestation of dogs with *Rhipicephalus sanguineus* (Acari: Ixodidae) in Hungary: Case report and review of current knowledge on this tick species. *Magyar Állatorvosok Lapja* 2015, 127, 623–629.
- [49] Földvári, G.; Szabó, É.; Tóth, G.E.; Lanszki, Z.; Zana, B.; Varga, Z.; Kemenesi, G. Emergence of *Hyalomma marginatum* and *Hyalomma rufipes* adults revealed by citizen science tick monitoring in Hungary. *Transbound. Emerg. Dis.* 2022, 69, e2240–e2248.. <https://doi.org/10.1111/tbed.14563>.
- [50] Földvári, G.; Rigó, K.; Jablonszky, M.; Biró, N.; Majoros, G.; Molnár, V.; Tóth, M. Ticks and the city: Ectoparasites of the Northern white-breasted hedgehog (*Erinaceus roumanicus*) in an urban park. *Ticks Tick-Borne Dis.* 2011, 2, 231–234. <https://doi.org/10.1016/j.ttbdis.2011.09.001>.
- [51] Hornok, S.; Csörgő, T.; de la Fuente, J.; Gyuranecz, M.; Privigyei, C.; Meli, M.L.; Kreizinger, Z.; Gönczi, E.; Fernández de Mera, I.G.; Hofmann-Lehmann, R. Synanthropic birds associated with high prevalence of tick-borne rickettsiae and with the first detection of *Rickettsia aeschlimannii* in Hungary. *Vector Borne Zoonotic Dis.* 2013, 13, 77–83. <https://doi.org/10.1089/vbz.2012.1032>.
- [52] Hornok, S.; Flaisz, B.; Takács, N.; Kontschán, J.; Csörgő, T.; Csipak, Á.; Jaksa, B.R.; Kováts, D. Bird ticks in Hungary reflect western, southern, eastern flyway connections and two genetic lineages of *Ixodes frontalis* and *Haemaphysalis concinna*. *Parasit. Vectors* 2016, 9, 101. <https://doi.org/10.1186/s13071-016-1365-0>.
- [53] Németh, V.; Oldal, M.; Egyed, L.; Gyuranecz, M.; Erdélyi, K.; Kvell, K.; Kalvatchev, N.; Zeller, H.; Bányai, K.; Jakab, F. Serologic evidence of Crimean-Congo hemorrhagic fever virus infection in Hungary. *Vector-Borne Zoonotic Dis.* 2013, 13, 270–272.

- [54] Földes, F.; Madai, M.; Németh, V.; Zana, B.; Papp, H.; Kemenesi, G.; Bock-Marquette, I.; Horváth, G.; Herczeg, R.; Jakab, F. Serologic survey of the Crimean-Congo haemorrhagic fever virus infection among wild rodents in Hungary. *Ticks Tick Borne Dis.* 2019, 10, 101258. doi: 10.1016/j.ttbdis.2019.07.002.
- [55] Blair, P.W.; Polanco-Ramos, A.; Kortepeter, M.; Kuhn, J.H.; Pecor, D.; Apanaskevich, D.; Rivard, R.; Keshtkar-Jahromi, M. Using the One Health Approach to Map Endemicity and Emergence of Crimean-Congo Hemorrhagic Fever in Europe, Southern and Western Asia. In *Proceedings of the ASTMH [American Society of Tropical Medicine and Hygiene] 66th Annual Meeting, Baltimore, MD USA, 5–9 November 2017.*
- [56] David Pecor: An Emerging, Tick-Borne Threat: CCHFV. A One Health Approach to Defining the Disease Burden of Crimean-Congo Hemorrhagic Fever Virus. *StoryMap.* 5 October 2023. Available online: <https://storymaps.arcgis.com/stories/3b4ef80e94164f83a0703ecf0c331914> (accessed on 9 April 2024).
- [57] Welch SR, Garrison AR, Bente DA, Burt F, D'Addiego J, Devignot S, Dowall S, Fischer K, Hawman DW, Hewson R, Mirazimi A, Oestereich L, Vatansever Z, Spengler JR, Papa A. Third International Conference on Crimean-Congo Hemorrhagic Fever in Thessaloniki, Greece, September 19-21, 2023. *Antiviral Res.* 2024 May;225:105844. doi: 10.1016/j.antiviral.2024.105844.
- [58] Jogtár: 18/1998. (VI. 3.) NM rendelet a fertőző betegségek és a járványok megelőzése érdekében szükséges járványügyi intézkedésekről. Available online: <https://net.jogtar.hu/jogszabaly?docid=99800018.nm> (last access 16 December 2024).
- [59] Kaya S, Elaldi N, Kubar A, Gursoy N, Yilmaz M, Karakus G, Gunes T, Polat Z, Gozel MG, Engin A, Dokmetas I, Bakir M, Yilmaz N, Sencan M. Sequential determination of serum viral titers, virus-specific IgG antibodies, and TNF- $\alpha$ , IL-6, IL-10, and IFN- $\gamma$  levels in patients with Crimean-Congo hemorrhagic fever. *BMC Infect Dis.* 2014 Jul 28;14:416. doi: 10.1186/1471-2334-14-416.

- [60] Papa A. Diagnostic approaches for Crimean-Congo hemorrhagic fever virus. *Expert Rev Mol Diagn.* 2019 Jun;19(6):531-536. doi: 10.1080/14737159.2019.1615450.
- [61] Ergunay K, Kocak Tufan Z, Bulut C, Kinikli S, Demiroz AP, Ozkul A. Antibody responses and viral load in patients with Crimean-Congo hemorrhagic fever: a comprehensive analysis during the early stages of the infection. *Diagn Microbiol Infect Dis.* 2014 May;79(1):31-6. doi: 10.1016/j.diagmicrobio.2013.12.015.
- [62] Sas MA, Comtet L, Donnet F, Mertens M, Vatansever Z, Tordo N, Pourquier P, Groschup MH. A novel double-antigen sandwich ELISA for the species-independent detection of Crimean-Congo hemorrhagic fever virus-specific antibodies. *Antiviral Res.* 2018 Mar;151:24-26. doi: 10.1016/j.antiviral.2018.01.006.
- [63] Johnson S, Henschke N, Maayan N, Mills I, Buckley BS, Kakourou A, Marshall R. Ribavirin for treating Crimean Congo haemorrhagic fever. *Cochrane Database Syst Rev.* 2018 Jun 5;6(6):CD012713. doi: 10.1002/14651858.CD012713.pub2.
- [64] European Virus Archive GLOBAL. Available online: <https://www.european-virus-archive.com> (last access 16 December 2024).
- [65] Sas MA, Vina-Rodriguez A, Mertens M, Eiden M, Emmerich P, Chaintoutis SC, Mirazimi A, Groschup MH. A one-step multiplex real-time RT-PCR for the universal detection of all currently known CCHFV genotypes. *J Virol Methods.* 2018 May;255:38-43. doi: 10.1016/j.jviromet.2018.01.013.
- [66] Vieyres G, Pietschmann T. Entry and replication of recombinant hepatitis C viruses in cell culture. *Methods.* 2013 Feb;59(2):233-48. doi: 10.1016/j.ymeth.2012.09.005.
- [67] Chrzastek K, Lee DH, Smith D, Sharma P, Suarez DL, Pantin-Jackwood M, Kapczynski DR. Use of Sequence-Independent, Single-Primer-Amplification (SISPA) for rapid detection, identification, and characterization of avian RNA viruses. *Virology.* 2017 Sep;509:159-166. doi: 10.1016/j.virol.2017.06.019.
- [68] Központi Statisztikai Hivatal (KSH): Interaktív korfa. Available online: <https://www.ksh.hu/interaktiv/korfak/orszag.html> (last access 16 December 2024).

- [69] European Centre for Disease Prevention and Control: European Map Maker. Available online: <https://mapmaker.ecdc.europa.eu> (last access 16 December 2024).
- [70] OpenStreetMap®. Available online: <https://data2.openstreetmap.hu/> (last access 16 December 2024).
- [71] Magyar N, Kis Z, Barabás É, Nagy A, Henczkó J, Damjanova I, Takács M, Pályi B. New geographical area on the map of Crimean-Congo hemorrhagic fever virus: First serological evidence in the Hungarian population. *Ticks Tick Borne Dis.* 2021 Jan;12(1):101555. doi: 10.1016/j.ttbdis.2020.101555.
- [72] Deézsi-Magyar N, Dénes B, Novák B, Zsidei G, Déri D, Henczkó J, Pályi B, Kis Z. First Broad-Range Serological Survey of Crimean-Congo Hemorrhagic Fever among Hungarian Livestock. *Viruses.* 2024 May 29;16(6):875. doi: 10.3390/v16060875.
- [73] Dai S, Wu Q, Wu X, Peng C, Liu J, Tang S, Zhang T, Deng F, Shen S. Differential Cell Line Susceptibility to Crimean-Congo Hemorrhagic Fever Virus. *Front Cell Infect Microbiol.* 2021 Mar 24;11:648077. doi: 10.3389/fcimb.2021.648077.
- [74] Connolly-Andersen AM, Douagi I, Kraus AA, Mirazimi A. Crimean Congo hemorrhagic fever virus infects human monocyte-derived dendritic cells. *Virology.* 2009 Aug 1;390(2):157-62. doi: 10.1016/j.virol.2009.06.010.
- [75] Connolly-Andersen AM, Moll G, Andersson C, Akerström S, Karlberg H, Douagi I, Mirazimi A. Crimean-Congo hemorrhagic fever virus activates endothelial cells. *J Virol.* 2011 Aug;85(15):7766-74. doi: 10.1128/JVI.02469-10.
- [76] Rodrigues R, Paranhos-Baccalà G, Vernet G, Peyrefitte CN. Crimean-Congo hemorrhagic fever virus-infected hepatocytes induce ER-stress and apoptosis crosstalk. *PLoS One.* 2012;7(1):e29712. doi: 10.1371/journal.pone.0029712.
- [77] Spengler JR, Kelly Keating M, McElroy AK, Zivcec M, Coleman-McCray JD, Harmon JR, Bollweg BC, Goldsmith CS, Bergeron É, Keck JG, Zaki SR, Nichol ST, Spiropoulou CF. Crimean-Congo Hemorrhagic Fever in Humanized Mice Reveals Glial Cells as Primary

Targets of Neurological Infection. *J Infect Dis.* 2017 Dec 12;216(11):1386-1397. doi: 10.3390/microorganisms8050775

[78] Földes K, Aligholipour Farzani T, Ergünay K, Ozkul A. Differential Growth Characteristics of Crimean-Congo Hemorrhagic Fever Virus in Kidney Cells of Human and Bovine Origin. *Viruses.* 2020 Jun 25;12(6):685. doi: 10.3390/v12060685.

[79] Agol VI. Cytopathic effects: virus-modulated manifestations of innate immunity? *Trends Microbiol.* 2012 Dec;20(12):570-6. doi: 10.1016/j.tim.2012.09.003.

[80] Rezelj VV, Levi LI, Vignuzzi M. The defective component of viral populations. *Curr Opin Virol.* 2018 Dec;33:74-80. doi: 10.1016/j.coviro.2018.07.014.

[81] Hardestam J, Simon M, Hedlund KO, Vaheri A, Klingström J, Lundkvist A. Ex vivo stability of the rodent-borne Hantaan virus in comparison to that of arthropod-borne members of the Bunyaviridae family. *Appl Environ Microbiol.* 2007 Apr;73(8):2547-51. doi: 10.1128/AEM.02869-06.

[82] D'Addiego J, Elaldi N, Wand N, Osman K, Bagci BK, Kennedy E, Pektas AN, Hart E, Slack G, Hewson R. Investigating the effect of ribavirin treatment on genetic mutations in Crimean-Congo haemorrhagic fever virus (CCHFV) through next-generation sequencing. *J Med Virol.* 2023. doi: 10.1002/jmv.28548.

[83] Kugelman JR, Wiley MR, Nagle ER, Reyes D, Pfeiffer BP, Kuhn JH, Sanchez-Lockhart M, Palacios GF. Error baseline rates of five sample preparation methods used to characterize RNA virus populations. *PLoS One.* 2017 Feb 9;12(2):e0171333. doi: 10.1371/journal.pone.0171333.

[84] Fitzpatrick AH, Rupnik A, O'Shea H, Crispie F, Keaveney S, Cotter P. High Throughput Sequencing for the Detection and Characterization of RNA Viruses. *Front Microbiol.* 2021 Feb 22;12:621719. doi: 10.3389/fmicb.2021.621719

[85] Parras-Moltó M, Rodríguez-Galet A, Suárez-Rodríguez P, López-Bueno A. Evaluation of bias induced by viral enrichment and random amplification protocols in metagenomic surveys of saliva DNA viruses. *Microbiome.* 2018 Jun 28;6(1):119. doi: 10.1186/s40168-018-0507-3.

- [86] Domingo E, Baranowski E, Ruiz–Jarabo CM, Martín-Hernández AM, Sáiz JC, Escarmís C. Quasispecies Structure and Persistence of RNA Viruses. *Emerg Infect Dis*. 1998;4(4):521-527. doi: 10.3201/eid0404.980402.
- [87] Ruedas JB, Arnold CE, Palacios G, Connor JH. Growth-Adaptive Mutations in the Ebola Virus Makona Glycoprotein Alter Different Steps in the Virus Entry Pathway. *J Virol*. 2018 Sep 12;92(19):e00820-18. doi: 10.1128/JVI.00820-18.
- [88] Ruedas JB, Ladner JT, Ettinger CR, Gummuluru S, Palacios G, Connor JH. Spontaneous Mutation at Amino Acid 544 of the Ebola Virus Glycoprotein Potentiates Virus Entry and Selection in Tissue Culture. *J Virol*. 2017 Jul 12;91(15):e00392-17. doi: 10.1128/JVI.00392-17.
- [89] Fay RL, Ngo KA, Kuo L, Willsey GG, Kramer LD, Ciota AT. Experimental Evolution of West Nile Virus at Higher Temperatures Facilitates Broad Adaptation and Increased Genetic Diversity. *Viruses*. 2021 Sep 22;13(10):1889. doi: 10.3390/v13101889.
- [90] Nemirov K, Lundkvist A, Vaheri A, Plyusnin A. Adaptation of Puumala hantavirus to cell culture is associated with point mutations in the coding region of the L segment and in the noncoding regions of the S segment. *J Virol*. 2003 Aug;77(16):8793-800. doi: 10.1128/jvi.77.16.8793-8800.2003.
- [91] Rahman SU, Yao X, Li X, Chen D, Tao S. Analysis of codon usage bias of Crimean-Congo hemorrhagic fever virus and its adaptation to hosts. *Infect Genet Evol*. 2018 Mar;58:1-16. doi: 10.1016/j.meegid.2017.11.027.
- [92] Chamberlain J, Cook N, Lloyd G, Mioulet V, Tolley H, Hewson R. Co-evolutionary patterns of variation in small and large RNA segments of Crimean-Congo hemorrhagic fever virus. *J Gen Virol*. 2005 Dec;86(Pt 12):3337-3341. doi: 10.1099/vir.0.81213-0.
- [93] Jenkins GM, Holmes EC. The extent of codon usage bias in human RNA viruses and its evolutionary origin. *Virus Res*. 2003 Mar;92(1):1-7. doi: 10.1016/s0168-1702(02)00309-x.
- [94] Plant EP, Ye Z. Bias at the third nucleotide of codon pairs in virus and host genomes. *Sci Rep*. 2022 Mar 16;12(1):4522. doi: 10.1038/s41598-022-08570-w

- [95] Fernandez-García, M.D., Negredo, A., Papa, A., Donoso-Mantke, O., Niedrig, M., Zeller, H., Tenorio, A., Franco, L., collective the ENIVD members, 2014. European survey on laboratory preparedness, response and diagnostic capacity for CrimeanCongo haemorrhagic fever, 2012. *Eurosurveillance* 19 (26) pii=20844. doi: 10.2807/1560-7917.es2014.19.26.20844.
- [96] Vanhomwegen, J., Alves, M.J., Zupanc, T.A., Bino, S., Chinikar, S., Karlberg, H., Korukluoglu, G., Korva, M., Mardani, M., Mirazimi, A., Mousavi, M., Papa, A., Saksida, A., Sharifi-Mood, B., Sidira, P., Tsergouli, K., Wolfel, R., Zeller, H., Dubois, P., 2012. Diagnostic assays for Crimean-Congo hemorrhagic fever. *Emerg. Infect. Dis.* 18 (12), 1958–1965. <https://doi.org/10.3201/eid1812.120710>.
- [97] Sidira P, Nikza P, Danis K, Panagiotopoulos T, Samara D, Maltezou H, Papa A. Prevalence of Crimean-Congo hemorrhagic fever virus antibodies in Greek residents in the area where the AP92 strain was isolated. *Hippokratia*. 2013 Oct;17(4):322-5.
- [98] Fajs L, Humolli I, Saksida A, Knap N, Jelovšek M, Korva M, Dedushaj I, Avšič-Županc T. Prevalence of Crimean-Congo hemorrhagic fever virus in healthy population, livestock and ticks in Kosovo. *PLoS One*. 2014 Nov 13;9(11):e110982. doi: 10.1371/journal.pone.0110982.
- [99] Sargianou, M., Panos, G., Tsatsaris, A., Gogos, C., Papa, A., 2013. Crimean-Congo hemorrhagic fever: seroprevalence and risk factors among humans in Achaia, western Greece. *Int. J. Infect. Dis.* 17 (12), e1160–1165. <https://doi.org/10.1016/j.ijid.2013.07.015>.
- [100] Chinikar, S., Goya, M.M., Shirzadi, M.-R., Ghiasi, S.M., Mirahmadi, R., Haeri, A., Moradi, M., Afzali, N., Rahpeyma, M., Zeinali, M., Meshkat, M., 2008. Surveillance and laboratory detection system of Crimean-Congo haemorrhagic fever in Iran. *Transbound. Emerg. Dis.* 55 (5–6), 200–204. <https://doi.org/10.1111/j.1865-1682.2008.01028.x>.
- [101] Bratuleanu B., Anita A., Temmam S., Dascalu A., Crivei L., Cozma A., Pourquier P., Savuta G., Eloit M., Anita D. Seroprevalence of Crimean-Congo Hemorrhagic Fever Among Small Ruminants from Southern Romania. *Vector Borne Zoonotic Dis.* 2022;22:397–401. doi: 10.1089/vbz.2021.0091

- [102] Mertens M, Vatansever Z, Mrenoshki S, Krstevski K, Stefanovska J, Djadjovski I, Cvetkovikj I, Farkas R, Schuster I, Donnet F, Comtet L, Tordo N, Ben Mechlia M, Balkema-Buschmann A, Mitrov D, Groschup MH. Circulation of Crimean-Congo Hemorrhagic Fever Virus in the former Yugoslav Republic of Macedonia revealed by screening of cattle sera using a novel enzyme-linked immunosorbent assay. *PLoS Negl Trop Dis.* 2015 Mar 5;9(3):e0003519. doi: 10.1371/journal.pntd.0003519.
- [103] Christova I, Panayotova E., Groschup M.H., Trifonova I, Tchakarova S., Sas M.A. High seroprevalence for Crimean-Congo haemorrhagic fever virus in ruminants in the absence of reported human cases in many regions of Bulgaria. *Exp. Appl. Acarol.* 2018;75:227–234. doi: 10.1007/s10493-018-0258-7.
- [104] Rehman K., Bettani M.A.K., Veletzky L., Afridi S., Ramharter M. Outbreak of Crimean-Congo haemorrhagic fever with atypical clinical presentation in the Karak District of Khyber Pakhtunkhwa, Pakistan. *Infect. Dis. Poverty.* 2018;7:116. doi: 10.1186/s40249-018-0499-z.
- [105] Balinandi S, Whitmer S, Mulei S, Nyakarahuka L, Tumusiime A, Kyondo J, Baluku J, Mutyaba J, Mugisha L, Malmberg M, Lutwama J, Shoemaker TR, Klena JD. Clinical and Molecular Epidemiology of Crimean-Congo Hemorrhagic Fever in Humans in Uganda, 2013-2019. *Am J Trop Med Hyg.* 2021 Oct 18;106(1):88-98. doi: 10.4269/ajtmh.21-0685.
- [106] Tsergouli K., Karampatakis T., Haidich A.B., Metallidis S., Papa A. Nosocomial infections caused by Crimean-Congo haemorrhagic fever virus. *J. Hosp. Infect.* 2020;105:43–52. doi: 10.1016/j.jhin.2019.12.001.
- [107] Nasirian H. Crimean-Congo hemorrhagic fever (CCHF) seroprevalence: A systematic review and meta-analysis. *Acta Trop.* 2019;196:102–120. doi: 10.1016/j.actatropica.2019.05.019.

## 9. Bibliography of publications

### Related publications

Deézsi-Magyar N, Dénes B, Novák B, Zsidei G, Déri D, Henczkó J, Pályi B, Kis Z. First Broad-Range Serological Survey of Crimean-Congo Hemorrhagic Fever among Hungarian Livestock. *Viruses*. 2024 May 29;16(6):875. doi: 10.3390/v16060875.

Magyar N, Kis Z, Barabás É, Nagy A, Henczkó J, Damjanova I, Takács M, Pályi B. New geographical area on the map of Crimean-Congo hemorrhagic fever virus: First serological evidence in the Hungarian population. *Ticks Tick Borne Dis*. 2021 Jan;12(1):101555. doi: 10.1016/j.ttbdis.2020.101555.

### Related book chapter

Magyar N. (2022): Chapter 27. *Nairoviridae*. In Takács M (Ed): *Orvosi Virologia (Medicina Kiadó)*. 2022;pp255-258.

### Non-related first and shared first author publications

Deézsi-Magyar N, Novák N, Lukács A, Tarcsai KR, Hajdu Á, Takács L, Farkas FB, Rigó Z, Barcsay E, Kis Z, Szomor K. First whole genome sequencing and analysis of human parechovirus type 3 causing a healthcare-associated outbreak among neonates in Hungary. *Eur J Clin Microbiol Infect Dis*. 2024 Dec;43(12):2341-2350. doi: 10.1007/s10096-024-04950-4.

Nóra M, Déri D, Veres DS, Kis Z, Barcsay E, Pályi B. Evaluating the field performance of multiple SARS-Cov-2 antigen rapid tests using nasopharyngeal swab samples. *PLoS One*. 2022 Feb 14;17(2):e0262399. doi: 10.1371/journal.pone.0262399.

Palyi B, Magyar N, Henczko J, Szalai B, Farkas A, Strecker T, Takacs M, Kis Z. Determining the effect of different environmental conditions on Ebola virus viability in clinically relevant specimens. *Emerg Microbes Infect*. 2018 Mar 29;7(1):52. doi: 10.1038/s41426-018-0043-z.

#### Non-related co-author publications

Nagy A, Horváth A, Mezei E, Henczkó J, Magyar N, Nagy O, Koroknai A, Csonka N, Takács M. West Nile virus infections in Hungary: Epidemiological update and phylogenetic analysis of the Hungarian virus strains between 2015 and 2022. *Acta Microbiol Immunol Hung*. 2023 May 2;70(2):111-118. doi: 10.1556/030.2023.02040.

Róka E, Déri D, Khayer B, Kis Z, Schuler E, Magyar N, Pályi B, Pándics T, Vargha M. SARS-CoV-2 variant detection from wastewater: rapid spread of B.1.1.7 lineage in Hungary. *J Water Health*. 2022 Feb;20(2):277-286. doi: 10.2166/wh.2022.179.

Róka E, Khayer B, Kis Z, Kovács LB, Schuler E, Magyar N, Málnási T, Oravecz O, Pályi B, Pándics T, Vargha M. Ahead of the second wave: Early warning for COVID-19 by wastewater surveillance in Hungary. *Sci Total Environ*. 2021 Sep 10;786:147398. doi: 10.1016/j.scitotenv.2021.147398.

Szalai B, Hercegh É, Magyar N, Déri D, Rózsa M, Molnár Z, Kuti D, Kis Z, Szomor K, Takács M, Barcsay E. A SARS-CoV-2 vírus magyarországi megjelenésének kimutatása légúti minták retrospektív vizsgálata alapján [Detection of the first appearance of SARS-CoV-2 virus in Hungary based on retrospective testing of respiratory samples]. *Orv Hetil*. 2020 Sep;161(38):1619-1622. Hungarian. doi: 10.1556/650.2020.32000.

Nagy A, Szöllősi T, Takács M, Magyar N, Barabás É. West Nile Virus Seroprevalence Among Blood Donors in Hungary. *Vector Borne Zoonotic Dis*. 2019 Nov;19(11):844-850. doi: 10.1089/vbz.2018.2401.

Carroll MW, Haldenby S, Rickett NY, Pályi B, Garcia-Dorival I, Liu X, Barker G, Bore JA, Koundouno FR, Williamson ED, Laws TR, Kerber R, Sissoko D, Magyar N, Di Caro A, Biava M, Fletcher TE, Sprecher A, Ng LFP, Rénia L, Magassouba N, Günther S, Wölfel R, Stoecker K, Matthews DA, Hiscox JA. Deep Sequencing of RNA from Blood and Oral Swab Samples Reveals the Presence of Nucleic Acid from a Number of Pathogens in Patients with Acute Ebola Virus Disease and Is Consistent with Bacterial Translocation

across the Gut. *mSphere*. 2017 Aug 23;2(4):e00325-17. doi:  
10.1128/mSphereDirect.00325-17.

#### Related international presentations

2023 Deézsi-Magyar N., Zsidei Gy., Novák B., Solymosi N., Kovanecz-Jármi L., Déri D., Pályi B., Kis Z.: Adaptation and genetic variations of the Crimean-Congo hemorrhagic fever virus resulted by in vitro serial passaging in different cell lines. In Molecular virology session. 3rd International Conference on Crimean-Congo hemorrhagic fever. 19-21 September, Thessaloniki, Greece.

2019 Magyar N., Palyi B., Henczkó J., Tóth Á., Kis Z.: Revealing the different adaptation mechanisms and genetic variations of the Crimean-Congo hemorrhagic fever virus using NGS. In Thomas Francis Jr. Semi-plenary Session. 18th International Congress of the Hungarian Society of Microbiology, 3-5 July, Budapest, Hungary.

2018 Magyar N., Palyi B., Barabas E., Nagy A., Henczko J., Damjanova I., Takacs M., Kis Z.: First serological evidence of Crimean–Congo haemorrhagic fever virus among Hungarian blood donors. In Session Emerging viruses, diagnostics and treatment. Power of Viruses Conference, 14-16 May, 2018, Porec, Croatia (with the support of the Federation of European Microbiological Societies Young Researcher Grant).

2017 Magyar N., Palyi B., Nagy A., Henczko J., Damjanova I., Barabas E., Takacs M., Kis Z.: First serological evidence of Crimean-Congo haemorrhagic fever virus in the Hungarian population. In Max Theiler Virology Session. 5th Central European Forum for Microbiology, 18-20 October 2017, Keszthely, Hungary.

#### Honors and awards during the course of the PhD training

2019-2020 Winner of the *New National Excellence Programme of the Hungarian Government* with the project "Investigation of the adaptation mechanism of the Crimean-Congo haemorrhagic fever virus using in vitro culture and next-generation sequencing methods".

2019 Best Poster Prize "The First Serosurvey of Crimean-Congo Hemorrhagic Fever Virus Focusing on Human and Animal Populations in Hungary" 1st Annual Scientific Meeting of the One Health European Joint Programme on food-borne zoonoses, antimicrobial resistance and emerging threats. May 22-24, 2019, Dublin, Ireland.

## 10. Acknowledgements

I am most grateful for my supervisors **Dr. Zoltán Kis** and **Bernadett Pályi** for their utmost help, patience and professional guidance during (and beyond) the course of my PhD program. Thank you for the many opportunities and support!

I would like to thank **my colleagues at the National Biosafety Laboratory** for their invaluable contribution, the endless BSL-4 working hours, and for all the memories created in the meantime. I am also thankful to **the colleagues at the Department of Microbiological Reference Laboratories** for their help in and out of the laboratory. I am also very grateful to all co-authors for their insightful and professional ideas and suggestions in our shared publications.

I am grateful to my family, especially my **husband Tamás** for making a calm and understanding atmosphere at home for me to be able to pursue and complete this thesis. I am also grateful for **my son, Nándi**, who taught me about next level patience. ☺

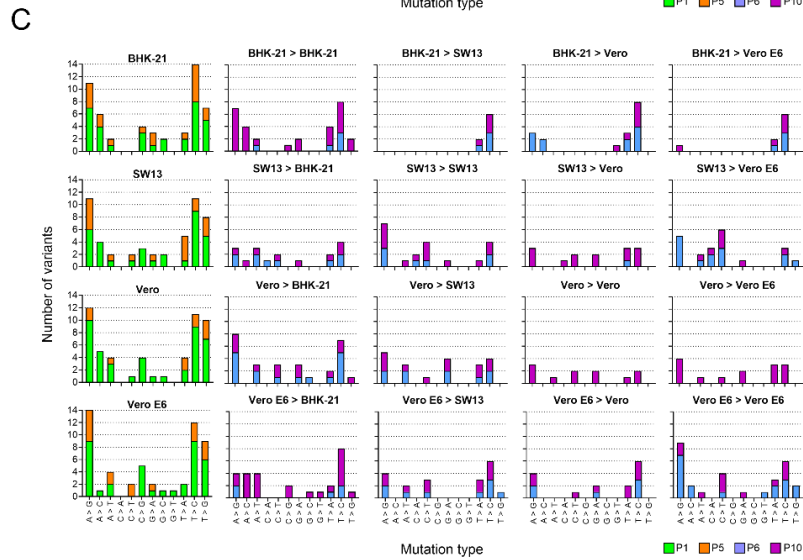
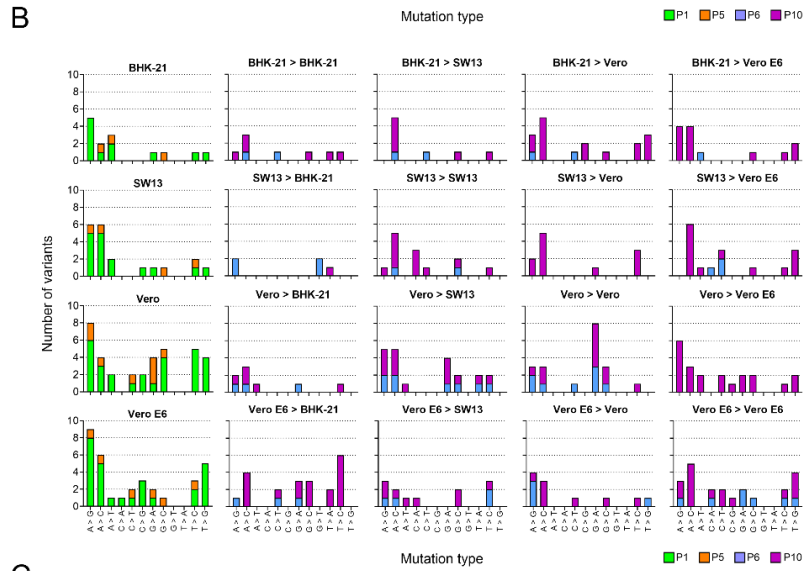
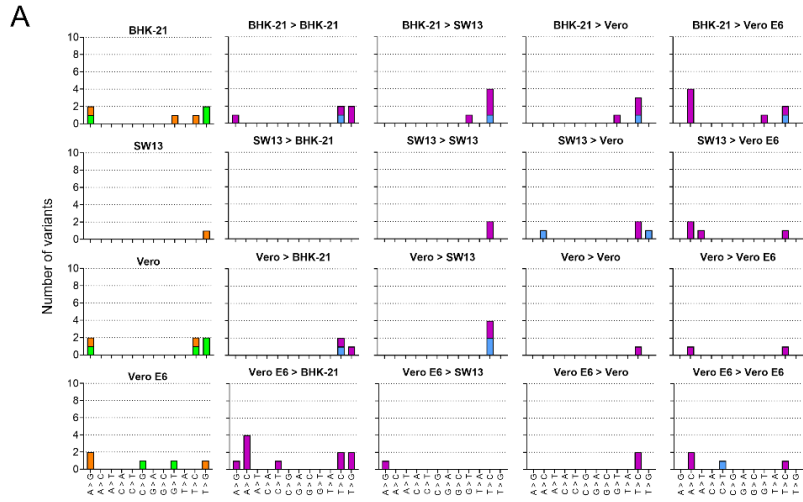
Finally, I would like to thank my parents for their endless support during my education and training, and for always encouraging me since I was a kid and for pushing me towards my limits. Thank you!

## 11. Appendix

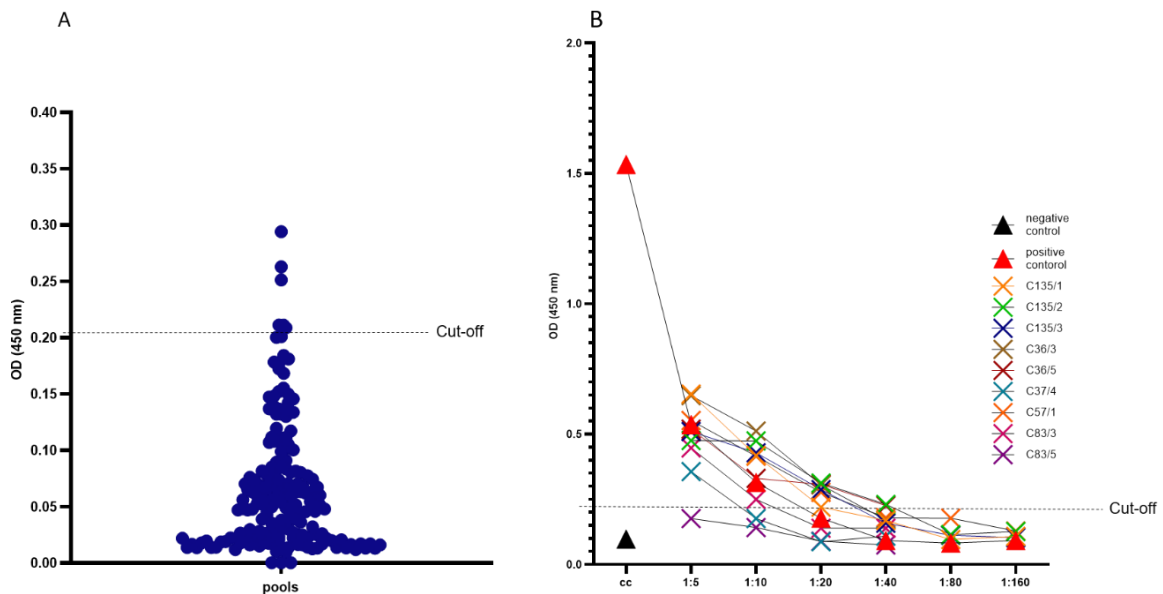
### 11.1. Figures



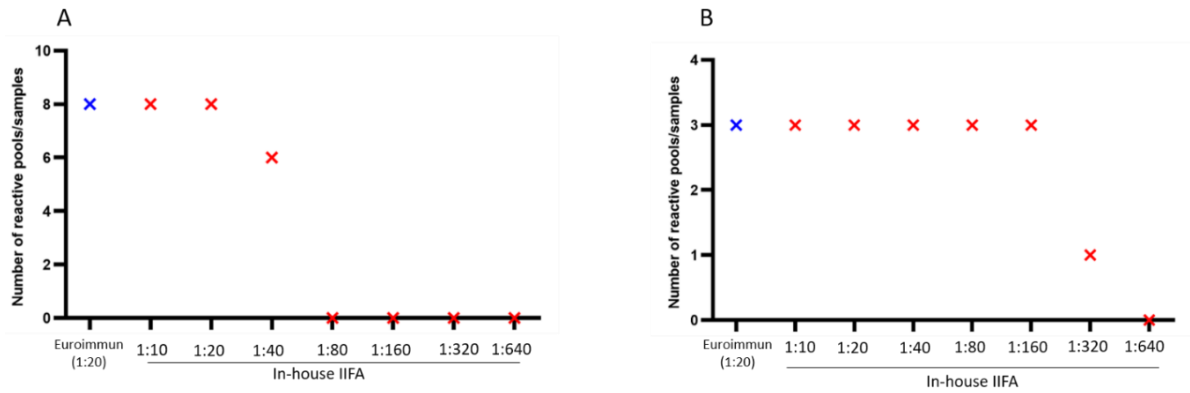
Appendix Figure 1. Our mutation accumulation study design. For the first passage (P1), suspensions of all four cell lines (at an initial  $3.0 \times 10^5$  cells/well density) were inoculated in three biological and three technical replicates using three different multiplicity of infection values (MOI 0.005, 0.01 and 0.1). Supernatant of each sample was collected directly after inoculation (day post infection; dpi 0), then in every 24 hours until day 7 (dpi 0-7). Based on virus growth, the optimal MOI (MOI = 0.005) and dpi for harvesting the supernatant were determined and used for the subsequent passages. After the first passage, the virus was further propagated in the same cell lines for an additional four passages (P1 - P5). Thereafter, the virus was further cross-passaged in every cell line for five additional times (P6 - P10). During the first cross-passage (P6) and the final passage (P10) the viral growth kinetics was also determined as described above. CCHFV whole genome sequencing was performed from the samples of P0, P1, P5, P6 and P10.



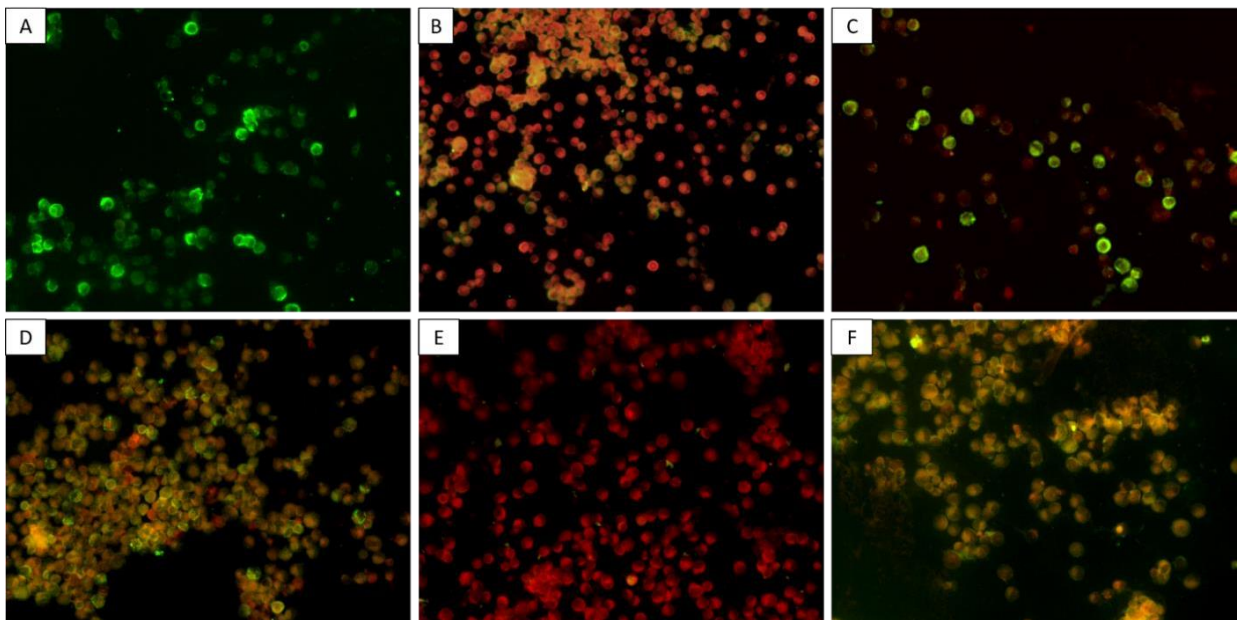
Appendix Figure 2. Nucleotide change preferences in the CCHFV genome induced by the host cell line by each segment: S (A), M (B) and L (C). Nucleotide change types are shown on the x-axis. First columns show the P1 (green) and P5 (orange) passage results by cell line. Columns 2-5 represent P6 (blue) and P10 (purple) cross-passages indicated as original cell line>new cell line: columns 2. Passaged to BHK-21, column 3. to SW13, column 4. to Vero, column 4. Vero E6 cells.



**Appendix Figure 3.** Results (OD values) obtained with Cow Crimean–Congo Hemorrhagic Fever Virus IgG (CCHF-IgG) ELISA kit for the **A.** pooled and **B.** individual samples of the reactive pools. ELISA testing was performed according to manufacturer’s instructions with pool samples diluted in 5-fold. Reactive individual samples were two-fold titrated (dilution range 1:5 – 1:160) and end-point titer was determined compared to cut-off OD to validate results. Read-out was performed at 450 nm. Cut-off value was determined as  $OD_{\text{negative control}} + 0.15$  according to the manufacturer’s instructions. Test is valid if  $OD_{\text{positive control}} \geq 1.0$ . Sample pools and individual samples with  $OD \geq$  cut-off value were considered reactive. OD values of the reactive samples (in dilution 1:5) were significantly higher compared to the OD of negative samples (unpaired t-test,  $P < 0.0001$ , GraphPad Prism 9.5.0 software).



Appendix Figure 4. Results obtained with the different immunofluorescent assays among **A**. cattle, **B**. sheep serum samples. Individual samples were diluted 1:20 for the EUROIMMUN IIFA testing. To determine the final anti-CCHF IgG antibody titer of the individual samples, two-fold serial dilution was tested in the range of 1:10 – 1:640 (shown on *x*-axis) using the in-house IIFA. Number of reactive samples at each dilution rate is shown in the graph (*y*-axis). Among the cattle samples, those that showed clear reactive results in all three tests were considered positive ( $n = 8$ ), and among the sheep samples, positivity was confirmed if reactivity was detected in both in-house and commercial IIFAs ( $n = 3$ ).



**Appendix Figure 5.** Detection of anti-CCHFV IgG with in-house (produced at the NCPHP NBL) IIFA slides containing whole-virus (CCHFV Afg09-2290 strain) infected Vero E6

cells. **A.** Reactive sheep sample pool (S86, dilution 1:20) with high background. Samples within the pool were tested further individually to verify anti-CCHFV IgG positivity. **B.** Negative sheep sample pool (dilution 1:20) with moderate background noise. **C.** Reactive sheep serum sample (S86/5, dilution 1:80). **D.** Positive cattle sample (C135/1, dilution 1:20). **E.** Negative cattle sample (dilution 1:20). **F.** Indeterminate cattle sample (C83/5, dilution 1:20) with high background, sample was discarded and concluded as seronegative. Immunofluorescence slides were stained with the respective secondary antibody (FITC-conjugated Anti-Sheep IgG (dilution 1:400) or FITC-conjugated Anti-Bovine IgG (dilution 1:300)). Fluorescence read-out was performed with the Leica DMI8 (Leica Microsystems, Wetzlar, Germany) microscope system. Images were processed with the LAS X Life Science Microscope Software (Leica Microsystems, Wetzlar, Germany) software. Fluorescence was evaluated for anti-CCHFV IgG-specific staining compared to the positive control (anti-CCHFV IgG positive polyclonal mouse serum) by two independent individuals. Photo: Leica DMI8 20x.

11.2. Tables

Appendix Table 1. Virus growth descriptive measures obtained during P1 in the different cell lines (maximum virus RNA copy number per mL, infective titer described as TCID50 per mL, and logarithmic increase in virus growth between dpi 0 and dpi with maximum virus RNA copy numbers and infective titers).

<b>P1</b>	<b>MOI 0.005</b>		<b>MOI 0.01</b>		<b>MOI 0.1</b>	
<b>Virus RNA copy number per mL</b>	<b>maximum</b>	<b>Logarithmic increase</b>	<b>maximum</b>	<b>Logarithmic increase</b>	<b>maximum</b>	<b>Logarithmic increase</b>
<b>Vero E6</b>	4.88E+08	2.49	5.03E+08	1.96	5.57E+08	1.43
<b>Vero</b>	1.25E+09	2.84	1.44E+09	2.48	1.62E+09	1.93
<b>SW13</b>	2.39E+09	2.84	1.62E+09	2.44	2.44E+09	1.80
<b>BHK-21</b>	8.23E+08	2.55	8.92E+08	1.91	7.13E+08	1.37
<b>TCID50 per mL</b>	<b>maximum</b>	<b>Logarithmic increase</b>	<b>maximum</b>	<b>Logarithmic increase</b>	<b>maximum</b>	<b>Logarithmic increase</b>
<b>Vero E6</b>	6.81E+03	3.83	1.47E+03	3.17	3.16E+03	1.00
<b>Vero</b>	3.16E+03	3.80	3.16E+03	3.50	3.16E+04	2.00
<b>SW13</b>	3.16E+04	4.50	6.81E+03	3.83	6.81E+04	2.33
<b>BHK-21</b>	4.47E+03	3.65	6.81E+03	3.83	3.16E+04	2.00
<b>Dpi with maximum TCID50 per mL</b>	<b>MOI 0.005</b>		<b>MOI 0.01</b>		<b>MOI 0.1</b>	
<b>Vero E6</b>	5		6		3	
<b>Vero</b>	6		7		3	
<b>SW13</b>	3		4		2	
<b>BHK-21</b>	4		3		2	

Appendix Table 2. Maximum virus RNA copy number per mL and maximum infective titer (TCID50 per mL) by original cell lines (P1-P5) and after the cross passages (P6-P10) to the new cell lines.

Maximum virus RNA copy number per mL								
new cells (P6-P10)	Vero E6				Vero			
original cells (P1-P5)	Vero E6	Vero	SW13	BHK-21	Vero E6	Vero	SW13	BHK-21
P1	5,43E+08					1,25E+09		
P6	2,77E+07	2,01E+08	2,41E+08	6,15E+08	1,31E+08	1,29E+08	2,16E+08	3,15E+08
P10	1,58E+08	2,74E+08	7,28E+07	3,08E+08	4,23E+08	4,09E+08	4,03E+08	4,23E+08
new cells (P6-P10)	SW13				BHK-21			
original cells (P1-P5)	Vero E6	Vero	SW13	BHK-21	Vero E6	Vero	SW13	BHK-21
P1			2,39E+09					9,67E+08
P6	1,13E+09	1,13E+09	9,90E+08	8,65E+08	2,62E+08	2,14E+08	1,98E+08	3,55E+08
P10	7,01E+08	7,01E+08	5,42E+08	1,62E+09	2,10E+08	2,36E+08	3,28E+08	1,81E+08
Maximum TCID50 per mL								
new cells (P6-P10)	Vero E6				Vero			
original cells (P1-P5)	Vero E6	Vero	SW13	BHK-21	Vero E6	Vero	SW13	BHK-21
P1	6,81E+04					6,81E+03		
P6	4,38E+02	4,38E+02	4,38E+02	4,38E+02	2,21E+03	2,21E+03	2,21E+03	2,21E+04
P10	7,01E+03	7,01E+03	1,21E+03	2,78E+04	2,72E+05	5,59E+04	2,72E+04	4,38E+03
new cells (P6-P10)	SW13				BHK-21			
original cells (P1-P5)	Vero E6	Vero	SW13	BHK-21	Vero E6	Vero	SW13	BHK-21
P1			3,16E+04					3,16E+03
P6	1,26E+04	3,16E+03	1,26E+03	2,12E+04	3,16E+03	3,16E+03	3,16E+03	1,26E+04
P10	4,38E+02	1,21E+03	6,44E+03	1,39E+04	5,59E+03	3,16E+03	2,33E+03	2,60E+03
dpi used for determination of infective titers (TCID50 per mL)								
new cells (P6-P10)	Vero E6				Vero			
original cells (P1-P5)	Vero E6	Vero	SW13	BHK-21	Vero E6	Vero	SW13	BHK-21
P1	5					6		
P6	6	5	5	5	6	6	7	7
P10	4	4	4	3	4	5	5	4
new cells (P6-P10)	SW13				BHK-21			
original cells (P1-P5)	Vero E6	Vero	SW13	BHK-21	Vero E6	Vero	SW13	BHK-21
P1			3					4
P6	3	4	2	2	4	6	4	4
P10	2	2	2	2	3	4	2	2

Appendix Table 3. Number of selected and tested serum samples by NUTS3 region, age group and gender based on the Hungarian demographic data obtained from the Hungarian Central Statistical Office website ([www.ksh.hu/interaktiv\\_korfa](http://www.ksh.hu/interaktiv_korfa)). F: female, M: male donors.

NUTS3 region	18-34y		35-50y		51-65y		Total
	M*	F*	M	F	M	F	
Bács-Kiskun	31	15	24	30	26	22	148
Baranya	22	12	21	21	29	11	116
Békés	16	15	16	15	16	15	93
Borsod-Abaúj-Zemplén	34	28	40	16	35	26	179
Budapest	84	84	73	76	83	97	497
Csongrád	18	21	20	16	19	20	114
Fejér	21	19	19	19	27	12	117
Győr-Moson-Sopron	22	18	27	17	23	13	120
Hajdu-Bihar	25	26	25	24	25	34	159
Heves	14	13	13	12	14	10	76
Jász-Nagykun-Szolnok	17	17	17	16	18	16	101
Komárom-Esztergom	19	8	15	13	13	9	77
Nógrád	9	8	9	9	9	8	52
Pest	44	54	60	53	75	26	312
Somogy	16	9	14	14	16	13	82
Szabolcs-Szatmár-Bereg	28	25	21	27	19	16	136
Tolna	12	8	10	13	10	9	62
Vas	18	11	11	21	16	7	84
Veszprém	12	19	23	8	18	11	91
Zala	18	12	17	9	17	11	84
<b>Total</b>	<b>480</b>	<b>422</b>	<b>475</b>	<b>429</b>	<b>508</b>	<b>386</b>	<b>2700</b>

Appendix Table 4. Detailed results of the reactive pools and individual samples by the initial screening and verification testing with ELISA or in-house IIFA testing. \* Cattle sample pools were screened with the Cow Crimean–Congo Hemorrhagic Fever Virus IgG (CCHF-IgG) ELISA Kit (Abbexa Ltd, Cambridge, United Kingdom). To test sheep samples pools, the in-house IIFA slides stained with FITC-conjugated Anti-Sheep IgG (whole molecule) were used. n.a.: not applicable

	<b>NUTS3 of origin</b>	<b>District of origin</b>	<b>ELISA/IIFA of the pool*</b>	<b>Pool and sample ID</b>	<b>ELISA result (titer)</b>	<b>in-house IIFA (titer)</b>	<b>Euroimmun IIFA</b>	<b>Final result</b>
<b>Cattle</b>	Pest	Monor	Equivocal	C127/1	negative	<1:20 negative	negative	negative
				C127/2	negative	<1:20 negative	negative	negative
				C127/3	negative	<1:20 negative	negative	negative
				C127/4	negative	<1:20 negative	negative	negative
				C127/5	negative	<1:20 negative	negative	negative
	Bács-Kiskun	Baja	Reactive	C135/1	1:20 reactive	1:40 reactive	reactive	positive
				C135/2	1:40 reactive	1:40 reactive	reactive	positive
				C135/3	1:20 reactive	1:40 reactive	reactive	positive
				C135/4	negative	<1:20 negative	indeterminate	negative
				C135/5	negative	<1:20 negative	negative	negative
	Győr-Moson-Sopron	Csorna	Reactive	C36/1	negative	<1:20 negative	negative	negative
				C36/2	negative	<1:20 negative	negative	negative

				C36/3	1:20 reactive	1:40 reactive	reactive	positive
				C36/4	negative	<1:20 negative	negative	negative
				C36/5	1:40 reactive	1:20 reactive	reactive	positive
	Győr- Moson- Sopron	Csorna	Equivocal	C37/1	negative	<1:20 negative	negative	negative
				C37/2	negative	<1:20 negative	negative	negative
				C37/3	negative	<1:20 negative	negative	negative
				C37/4	1:5 reactive	1:20 reactive	reactive	positive
				C37/5	negative	<1:20 negative	negative	negative
	Veszprém	Várpalota	Equivocal	C57/1	1:20 reactive	1:40 reactive	reactive	positive
				C57/2	negative	<1:20 negative	negative	negative
	Csongrád	Csongrád	Equivocal	C83/1	negative	<1:20 negative	negative	negative
				C83/2	negative	<1:20 negative	negative	negative
				C83/3	1:10 reactive	1:40 reactive	reactive	positive
				C83/4	negative	<1:20 negative	negative	negative
				C83/5	negative	<1:20 negative	indeterminate	negative
Sheep	Bács- Kiskun	Kiskunfélegyháza	Reactive	S86/1	n.a.	1:160 reactive	reactive	positive
				S86/2	n.a.	<1:20 negative	negative	negative

				S86/3	n.a.	<1:20 negative	negative	negative
				S86/4	n.a.	1:160 reactive	reactive	positive
				S86/5	n.a.	1:320 reactive	reactive	positive